Pergamon

Geochimica et Cosmochimica Acta, Vol. 66, No. 4, pp. 595–614, 2002

0016-7037/−1898 $22.00 + .00

PII S0016-7037(00)00798-0

Strontium isotope composition of runoff from a glaciated carbonate terrain

MARTIN SHARP,[1] ROBERT A. CREASER,[1] and MARK SKIDMORE[1,2]

[1]Department of Earth and Atmospheric Sciences, University of Alberta, Edmonton, Alberta T6G 2E3, Canada
[2]Bristol Glaciology Centre, School of Geographical Sciences, University of Bristol, Bristol BS8 1SS, United Kingdom

(*Received June* 27, 2001; *accepted in revised form July* 31, 2001)

Abstract—The relationship between subglacial chemical weathering processes and the Sr isotope composition of runoff from Robertson Glacier, Alberta, Canada, is investigated. This glacier rests on predominantly carbonate bedrock of Upper Devonian age, but silicate minerals are also present. The provenance of solute in meltwaters is found to vary systematically with solute concentration and, by inference, subglacial water residence time. In dilute waters, the principal process of solute acquisition is calcite dissolution fueled by protons derived from the dissolution of CO_2 and subsequent dissociation of carbonic acid. At higher solute concentrations, dolomite dissolution coupled to sulfide oxidation is more important. Sr concentration is found to increase with total solute concentration in two separate meltwater streams draining from the glacier, but $^{87}Sr/^{86}Sr$ only increases in the eastern melt stream. Carbonate and K-feldspar sources are shown to dominate the Sr content of the western stream, irrespective of concentration. They also dominate the Sr content of the eastern stream at low and intermediate concentrations, but at higher concentrations, muscovite (with high $^{87}Sr/^{86}Sr$) is also an important Sr source. This reflects the outcrop of muscovite-bearing lithologies in the catchment of the eastern stream and an increase in the rate of weathering of K-silicates relative to that of carbonates as more concentrated solutions approach saturation with respect to carbonates. Nonstoichiometric release of $^{87}Sr/^{86}Sr$ and preferential release of Sr over K from freshly ground K-silicate surfaces may also occur. This may help to explain the radiogenic nature of runoff from distributed subglacial drainage systems, which are characterized by long water:rock contact times and water flow through environments in which crushing and grinding of bedrock are active processes.

Although the exchangeable Sr in tills has higher $^{87}Sr/^{86}Sr$ than local carbonate bedrock, only the more concentrated meltwaters from the eastern stream display similarly high values. The most dilute waters, which probably transport the bulk of the dissolved Sr flux from the glacier, have $^{87}Sr/^{86}Sr$ characteristic of local carbonate bedrock. Thus, the results suggest that although enhanced weathering of silicate minerals containing radiogenic Sr (such as muscovite) does occur in glaciated carbonate terrains, it is unlikely to contribute to any enhanced flux of radiogenic Sr from glaciated continental surfaces to the oceans. *Copyright © 2002 Elsevier Science Ltd*

1. INTRODUCTION

Over the last 40 Ma, the marine $^{87}Sr/^{86}Sr$ ratio has increased dramatically from ~0.7078 to the current value of 0.70925 (Burke et al., 1982; Capo and DePaolo, 1990; Edmond, 1992; Richter et al., 1992). This increase is widely attributed to an increase in the delivery of radiogenic Sr to the oceans from the continents. This is because the $^{87}Sr/^{86}Sr$ ratio of continental runoff is significantly higher than that of other major Sr fluxes to the ocean (hydrothermal sources and deep-sea sediment pore waters), and because the fluxes of Sr from such sources have varied little through late Cenozoic time (Palmer and Edmond, 1989).

The proposed increase in continental Sr fluxes has been taken to indicate an increase in the rate of continental chemical weathering during the late Cenozoic. Possible causes of this increase include Himalayan uplift and the increasing extent of continental glaciation (Raymo et al., 1988; Hodell et al., 1990; Raymo and Ruddiman, 1992; Richter et al., 1992; Blum and Erel, 1995; Zachos et al., 1999). Himalayan uplift has attracted particular attention because Himalayan rivers are characterized by both high Sr concentrations and high values of $^{87}Sr/^{86}Sr$ (Palmer and Edmond, 1989; Krishnaswami et al., 1992; Richter et al., 1992). It has been argued that enhancement of silicate weathering by Himalayan uplift contributed to late Cenozoic global cooling by drawing down atmospheric CO_2 (Raymo and Ruddiman, 1992). However, it is not clear whether the radiogenic Sr transported by Himalayan rivers is derived from silicate or carbonate sources (Edmond, 1992; Krishnaswami et al., 1992; Quade et al., 1997; Blum et al., 1998; Harris et al., 1998; Singh et al., 1998; English et al., 2000; Karim and Veizer, 2000). This issue is important because carbonate weathering would not result in long-term drawdown of atmospheric CO_2 and could thus not be implicated in late Cenozoic cooling.

Moreover, it is not clear that an increase in the flux of radiogenic Sr from the continents necessarily implies an increase in continental weathering rates. The observed change in marine $^{87}Sr/^{86}Sr$ could also arise from a change in the isotopic composition of continentally derived Sr (Richter et al., 1992; Harris, 1995; Derry and France-Lanord, 1996; Quade et al., 1997; Chesley et al., 2000; English et al., 2000). Several workers have demonstrated that changes in the $^{87}Sr/^{86}Sr$ of Himalayan runoff have in fact occurred during the late Cenozoic (Derry and France-Lanord, 1996; Quade et al., 1997; Chesley et al., 2000; English et al., 2000). Possible causes of such a change include the following: (1) a shift in the balance

* Author to whom correspondence should be addressed (martin.sharp@ualberta.ca).

of lithologies being weathered due to, for instance, the effects of uplift on the exposure of different lithologies to chemical weathering (Harris, 1995; Quade et al., 1997; English et al., 2000); (2) a change in the intensity of continental chemical weathering (Derry and France-Lanord, 1996; Zachos et al., 1999); and (3) development of a continental weathering regime that selectively weathers trace components of the bedrock with relatively high $^{87}Sr/^{86}Sr$ ratios (such as biotite; Blum et al., 1994, 1998; Blum and Erel, 1995), or results in nonstoichiometric release of $^{87}Sr/^{86}Sr$ from minerals (Brantley et al., 1998).

Several workers have postulated links between the marine $^{87}Sr/^{86}Sr$ record and changes in the extent of continental glaciation (Hodell et al., 1990; Zachos et al., 1999), and these could be explained by any or all of the three effects listed above. Continental glaciation could change the balance of lithologies being weathered by altering the rate of weathering of continental surfaces that become glaciated. Because continental ice sheets developed on ancient shield terrains that currently yield runoff with high values of $^{87}Sr/^{86}Sr$ (0.8 to 0.9; Wadleigh et al., 1985), this could have had a significant impact on the mean $^{87}Sr/^{86}Sr$ of continental runoff (Edmond, 1992; Palmer and Edmond, 1992). Glaciation could also have produced a change in continental weathering regime. Active subglacial crushing and grinding of bedrock continually renew the supply of trace components of bedrock and generate ultrafine particles with damaged surfaces that are highly reactive (Blum and Erel, 1995; Anderson et al., 1997, 2000; Brantley et al., 1998). Such reactive trace components include minerals, such as biotite, that have very high $^{87}Sr/^{86}Sr$ (Blum and Erel, 1997). These trace phases may have a disproportionate influence on the Sr isotope systematics of glacial runoff. Consistent with this suggestion are observations in recently glaciated silicate terrains that show that both the exchangeable Sr pool in tills and base-flow runoff have elevated $^{87}Sr/^{86}Sr$ values relative to local bedrock (Blum et al., 1994; Blum and Erel, 1995, 1997). Because biotite alteration may proceed even more rapidly in subglacial environments than in recently deposited glacial sediments (Anderson et al., 2000), selective glacial weathering of radiogenic trace phases may have a considerable influence on the Sr isotope composition of continental runoff (Blum and Erel, 1995). To date, however, there have been too few detailed investigations of the Sr isotope systematics of glacial runoff to evaluate this hypothesis.

Studies of the major ion composition of glacial runoff suggest that carbonate weathering tends to dominate the solute load of glacial meltwaters (Anderson et al., 2000; Tranter et al., in press). This is true even in silicate terrains where carbonates occur only as trace components of the bedrock (Clow et al., 1997; Blum et al., 1998; Anderson et al., 2000; Tranter et al., in press). However, the chemistry of glacial runoff shows large changes over the course of a melt season as a result of changes in flow routing and subglacial water:rock contact times, and of the different reaction kinetics of carbonate, sulfide, and silicate minerals (Brown et al., 1996). Evaluation of the effects of glaciation on the discharge-weighted mean $^{87}Sr/^{86}Sr$ of continental runoff demands an understanding of the implications of these changes for the Sr isotopic composition of glacial runoff and its relationship to that of local bedrock. Investigations of these effects need to be conducted in both carbonate and silicate terrains.

This article discusses the relationship between subglacial chemical weathering processes and the Sr isotope systematics of meltwater runoff from Robertson Glacier, Alberta, Canada. This glacier rests on predominantly carbonate bedrock, but the carbonates contain significant amounts of K-silicate minerals that are expected to have relatively high $^{87}Sr/^{86}Sr$. The aims of this article are the following: (1) to use the major ion chemistry of runoff to determine how variations in water flux and subglacial water residence time affect the balance of mineral phases being weathered beneath the glacier; (2) to determine the relationships between solute sources and the isotopic composition of Sr dissolved in the meltwaters; and (3) to determine whether release of Sr from silicate minerals occurs within this predominantly carbonate catchment, and assess whether it is an important enough process to raise the discharge-weighted mean $^{87}Sr/^{86}Sr$ ratio of meltwater runoff above that of local carbonate bedrock.

2. STUDY SITE DESCRIPTION

Robertson Glacier (115°20′W, 50°44′N) drains the northern flank of the Haig Icefield in Peter Lougheed Provincial Park, Kananaskis Country, Alberta, Canada. The glacier is approximately 3 km long and spans an elevation range from 2900 to 2370 m. It currently terminates on a flat till plain, although glacially smoothed bedrock surfaces are exposed along the glacier margins. Some of these bedrock surfaces carry a veneer of subglacially precipitated calcite (Hallet, 1976) and are incised by discontinuous “Nye channels” (Walder and Hallet, 1979). Two principal subglacial meltwater streams, referred to here as RE (eastern) and RW (western), drain from beneath the ice front. RE shows a more flashy hydrological response to summer diurnal melt cycles than RW. The local bedrock is Upper Devonian in age (Mount Hawk, Palliser and Sassenach Formations) and consists of impure limestones, dolostones, and dolomitic limestones, with interbeds of shale, siltstone, and sandstone (McMechan, 1988).

3. SAMPLING AND ANALYTICAL METHODS

Two samples of till were collected from the till plain immediately in front of the glacier, and 21 bedrock samples were taken from outcrops in the proglacial area and on the valley walls. Bedrock sampling included all the major lithologies that are likely to crop out on the current glacier bed. Whole-rock samples were crushed (avoiding weathered surfaces and chips) and then milled in steel to achieve a fine powder. The mineralogy of 1 till sample and 13 bedrock powders was determined by X-ray diffraction, whereas the elemental composition of 7 bedrock powders was determined by instrumental neutron activation analysis (INAA) in the University of Alberta Slowpoke Reactor facility. The bedrock samples analyzed were representative of the major lithologies that were sampled.

Before Sr isotope analysis, bedrock powders were treated by various leaching and dissolution protocols to allow investigation of the Sr isotope composition of the major mineral phases in the bedrock. These leaches were performed in the Radiogenic Isotope Facility, Department of Earth and Atmospheric Sciences, University of Alberta, under class 100 (or better)

clean room conditions. All acids used were purified by subboiling distillation in Teflon Perfluoralkoxy (PFA) stills. Total procedural blanks for Sr are 100 to 200 pg and are insignificant relative to the amount of Sr analyzed for any sample.

Two separate hydrochloric acid leaches, designed to dissolve all carbonate material (calcite and dolomite), were performed. Twelve whole-rock samples were dissolved in 1.0 N hydrochloric acid at room temperature (23°C) for 12 h (HCl (1) in Table 3). Three of these (R1, 5, 18) were also dissolved in 0.1 N hydrochloric acid at room temperature for 2 h (HCl (2) in Table 3). In both cases, the supernate was removed, filtered, and reserved for Sr isotopic analysis. An additional series of three sequential leaches was performed on these three samples. Leach 1 used 1.7 N acetic acid at room temperature for 10 min and was designed to maximize dissolution of calcite relative to dolomite (Cavell, personal communication). The sample was then centrifuged and the supernate removed with a precleaned, fine-tipped disposable pipette, dried in a laminar flow HEPA-filtered exhaust enclosure, and reserved for Sr isotopic analysis. The remaining material was washed twice with ~5 mL 18.2 MΩ water and centrifuged, and the supernate was discarded. The washed residue was leached again with 1.7 N acetic acid at room temperature for 120 min (leach 2) and centrifuged, and the supernate was again dried and reserved for Sr isotopic analysis. This step was designed to maximize dissolution of dolomite (Cavell, personal communication). The residue was again washed twice with ~5 mL 18.2 MΩ water and centrifuged, and the supernate was discarded. The remaining undissolved silicate material was then reacted with a 5:2 mix of 24 N hydrofluoric acid plus 16 N nitric acid in a sealed Teflon PFA vessel at 160°C for 24 h (leach 3). After drying, the fluoride residue was reacted with 6.2 N hydrochloric acid and again dried before Sr isotopic analysis. Leach 1 was also performed on 5 additional samples (R3, 4, 7, 12, 20). To determine the isotopic composition of Sr from the exchangeable cation pool in the tills, two samples were reacted with ~1 mol/L ammonium acetate for 5 min at 23°C. The supernate was removed and reserved for Sr isotopic analysis. Because ammonium acetate can dissolve carbonates (Tessier et al., 1979), which have a lower isotopic ratio than the exchangeable Sr (see below), the isotopic ratios derived by this procedure should be regarded as minimum estimates of the true composition of the exchangeable Sr.

Samples of meltwater were collected from both RE and RW on 12 dates between June 22 and October 21, 1995. On eight of these dates, samples were collected at different stages of the diurnal discharge hydrograph. In addition, a single sample was collected from a supraglacial stream with the aim of characterizing the chemical composition of initial ice melt. Immediately after collection, water samples were vacuum filtered through 0.45-μm cellulose nitrate membranes. Twenty-milliliter aliquots were collected in polyethylene scintillation vials that had been prerinsed with filtered sample for analysis of their major cation and anion content by ion chromatography, and of their dissolved silica content by flow injection. The cation sample was acidified by 750 μL of 1 M methanesulfonic acid. For anions, precision and accuracy were better than ±6% at concentrations >3 μEq L^{-1}. For cations, they were better than ±8% at concentrations > 2 μEq L^{-1}. At concentrations >1 μmol L^{-1}, silica determinations had an accuracy better than ±6% and precision better than ±8%. In addition, pH, alkalinity, and electrical conductivity were measured in the field immediately after filtration. pH was measured with an Orion 290A pH meter that was calibrated with Orion low ionic strength buffers (4.1 and 6.97). Alkalinity was measured by colorimetric titration to end point pH 4.5 with 0.16 N sulfuric acid titrant and a Hach digital titrator.

Aliquots (250 mL) of selected samples were collected for measurement of their dissolved Sr content and its isotopic composition by thermal ionization–isotope dilution mass spectrometry. Samples were filtered as described above and collected in polyethylene bottles. These were precleaned by performing two repetitions of the following procedure: (1) triple rinse in 18.2 MΩ water, (2) filled with 18.2 MΩ water and left to stand for 3 d, and (3) emptied and triple rinsed in 18.2 MΩ water. After collection, samples were acidified with 800 μL of 6.2 N purified HCl. For Sr isotope analysis, ~40 g of water from each sample was accurately weighed and spiked with a known amount of ^{84}Sr tracer solution. The tracer solution has been calibrated directly against a gravimetrically prepared solution of the Sr reference material SRM987, and the concentration of ^{84}Sr is known to better than ±0.2%. The spiked solutions were then dried ready for analysis. Chemical separation and mass analysis of Sr used standard cation exchange chromatography and thermal ionization mass spectrometry (Holmden et al., 1996), except that Sr was loaded onto a single rhenium filament together with a mixture of hydrous tantalum pentoxide gel and orthophosphoric acid. This is a high-sensitivity technique which allows analysis of as little as 6 ng total Sr. All $^{87}Sr/^{86}Sr$ analyses are corrected for variable mass fractionation to $^{86}Sr/^{88}Sr = 0.1194$ and are presented relative to $^{87}Sr/^{86}Sr = 0.710245$ for SRM987 to facilitate interlaboratory comparison. The values for the SRM987 standard analyzed over the course of the study yielded an average value of 0.71021 ± 0.00003 (1 standard deviation).

In addition, in September 1996, two 4-L samples were collected for analysis of $\delta^{34}S\text{-}SO_4$ and $\delta^{18}O\text{-}SO_4$. These samples were vacuum filtered through 0.45-μm cellulose nitrate filter membranes into opaque polyethylene bottles and stored at 4°C. In the laboratory, they were passed through anion exchange resin to collect the SO_4. Extraction of the SO_4 from the ion exchange columns and isotopic analysis on a VG Micromass 602D dual collector mass spectrometer were performed at the Environmental Isotope Laboratory, University of Waterloo (for full details of methods, see Heemskerk, 1993a,b).

4. RESULTS

4.1. Mineralogy and Geochemistry of Bedrock and Till Samples

The primary mineral phases in the bedrock are calcite and dolomite, although many samples also contain some quartz, K-feldspar, and muscovite. Illite and bassinite are also present in the till sample analyzed, and pyrite is clearly visible in many bedrock samples. INAA analyses (Table 1) confirm the presence of significant amounts of K-silicates and show that Na is present at much lower levels than K in bedrock. Sr concentrations range from 39 to 360 ppm and correlate positively with Ca and inversely with K (Table 2). By contrast, Rb concentrations range from 4 to 83 ppm and correlate positively with K,

Table 1. Results of X-ray diffraction and INAA analyses of bedrock samples from Robertson Glacier.[a]

Sample	Mineralogy	Ca (%)	K (%)	Na (%)	Al (%)	Fe (%)	Rb (ppm)	Sr (ppm)	K/Rb
R4	C D Q	15.7	1.93	0.04	2.5	1.2	52	175	371
R7	C Q	32.4	0.2	0.02	0.16	0.6	4.2	360	476
R8	C D Q Mu	9.1	2.8	0.22	3.52	1.8	83	108	337
R9	C D Q O Mi	10.4	2.29	0.11	2.5	1.4	66	120	347
R14	C D Q	8	2.03	0.14	2.2	1	59	62	344
R16	C D Q S	10.5	1.9	0.44	1.9	0.6	50	120	380
R20	C D Q	5.7	1.71	0.04	1.3	0.7	32	39	534

[a] For mineralogy, C = calcite; D = dolomite; Q = quartz; Mu = muscovite; Mi = microcline; O = orthoclase; S = sanidine.

Al, and Fe and inversely with Ca and Sr. These relationships suggest that most Sr is contained within carbonate minerals, whereas Rb is found mainly in K-feldspar and muscovite.

The K/Rb ratios of the samples range from 337 to 534. K/Rb ratios in K-feldspars from granitic rocks range from ~100 to 600 and average ~300 (Speer, 1984), whereas K/Rb ratios in micas (igneous biotite and muscovite) are generally less than 150 (Cerny and Burt, 1984; Speer, 1984). These observations suggest that the K/Rb ratios of the bedrock samples are dominated by K-feldspar rather than by muscovite.

4.2. Strontium Isotopes in Bedrock and Till

Sr derived from the silicate fraction of the bedrock has a significantly higher $^{87}Sr/^{86}Sr$ ratio than carbonate-derived Sr (Table 3). This is consistent with much of the silicate-derived Sr being produced by radioactive decay of ^{87}Rb to ^{87}Sr in minerals with significantly higher Rb/Sr than carbonate. The mean $^{87}Sr/^{86}Sr$ ratio of calcite is slightly higher than that of dolomite. However, the calcite ratios have a bimodal distribution (four of the eight samples analyzed produced $^{87}Sr/^{86}Sr$

Table 2. Correlation matrix for elemental abundances in samples of bedrock from Robertson Glacier (as derived from INAA analyses).[a]

Variable	Ca (%)	K (%)	Na (%)	Al (%)	Fe (%)	Rb (ppm)	Sr (ppm)
Ca (%)	1.00	−0.84*	−0.36	−0.65	−0.33	−0.70	0.99*
K (%)	−0.84*	1.00	0.40	0.95*	0.75	0.97*	−0.78*
Na (%)	−0.36	0.40	1.00	0.34	−0.03	0.41	−0.29
Al (%)	−0.65	0.95*	0.34	1.00	0.87*	0.98*	−0.58
Fe (%)	−0.33	0.75	−0.03	0.87*	1.00	0.83*	−0.26
Rb (ppm)	−0.70	0.97*	0.41	0.98*	0.83*	1.00	−0.64
Sr (ppm)	0.99*	−0.78*	−0.29	−0.58	−0.26	−0.64	1.00

[a] Significant correlations ($p = 0.05$) are marked with an asterisk.

Table 3. Sr isotopic results of leaching experiments on samples of bedrock and till from Robertson Glacier.[a] Uncertainty (fifth decimal place) of analyses is given in brackets after isotopic ratios.

Sample	Mineralogy	$^{87}Sr/^{86}Sr$ HCl (1) carbonate	$^{87}Sr/^{86}Sr$ HCl (2)	$^{87}Sr/^{86}Sr$ Acetic 1 (calcite)	$^{87}Sr/^{86}Sr$ Acetic 2 (dolomite)	$^{87}Sr/^{86}Sr$ HF/HNO^3 (silicate)	$^{87}Sr/^{86}Sr$ NH_4 Ac
R3	Q C D Mu	0.70995 (2)		0.70989 (2)			
R4	Q C D	0.71026 (2)		0.71013 (1)			
R5	Q C D Mu	0.71034 (2)	0.71035 (2)	0.71039 (2)	0.70963 (2)	0.79559 (2)	
R7	Q C	0.70860 (2)		0.70845 (2)			
R8	Q C D Mu	0.71084 (2)					
R9	Q C D O Mi	0.71011 (2)					
R12	Q C D	0.70923 (2)		0.70906 (1)			
R14	Q C D	0.71073 (2)					
R1	Q C D S	0.70873 (2)	0.70872 (2)	0.70866 (2)	0.70857 (2)	0.75351 (2)	
R17	Q C D S	0.70901 (2)					
R18	Q C D S	0.70905 (2)	0.70906 (2)	0.70892 (2)	0.70884 (1)	0.76385 (2)	
R20	Q C D	0.71056 (2)		0.71058 (2)			
Till	Q C D I B						0.71030 (2)
Till	Not analyzed						0.71020 (2)
Mean		0.70978	0.70938	0.70951	0.70901	0.77098	0.71025
Standard deviation	0.00081	0.00086	0.00083	0.00055	0.02193	0.00007	

[a] 2σ Mineralogy: Q = quartz; C = calcite; D = dolomite; Mu = muscovite; Mi = microcline; O = orthoclase; S = sanidine; I = illite; B = bassinite. Details of the leaching procedures are given in text.

Table 4. Chemical characteristics of meltwaters from a supraglacial stream (n = 1) and from the two melt streams (RE and RW) draining Robertson Glacier, Alberta.[a]

Element	Supra glacial	RE Mean	RE SD	RE CV %	RW Mean	RW SD	RW CV %	Ratio of Means	Ratio of CV
Ca^{2+}	126	959.4	943.7	98.3	1124.3	666.7	59.3	0.85	1.66
Mg^{2+}	8.1	290	516.4	178	313.4	280.7	89.6	0.93	1.99
Na^{+}	5.8	3.7	4.5	121.5	3.6	4.5	125.6	1.03	0.9
K^{+}	3.2	9.2	18.4	201	5.8	4.4	75.4	1.58	2.6
Si	0.2	3.0	2.2	71.9	5.4	1.5	27.3	0.56	2.63
HCO_3^{-}	131	885	612.3	69.2	924.9	397.6	63	0.96	1.1
SO_4^{2-}	5	376.6	880	233.6	520.1	563.2	108.3	0.72	2.16
CI^{-}	6.1	2.5	3.3	130	1.7	0.8	49.7	1.47	2.62
Sr^{2+}	N.D.	1.6	2.4	147.4	2.9	4.8	168	0.57	0.88
SEF	0.037	0.18	0.12	68.4	0.31	0.09	28.4	0.58	2.4
Ca^{2+}/Mg^{2+}	15.6	5.7	3.2	56.9	4.1	0.83	20.5	1.39	2.78
Si/K^{+}	0.06	0.55	0.27	50	1.14	0.42	36	0.48	1.39
$^{87}Sr/^{86}Sr$	N.D.	0.70985	0.00041	0.06	0.70971	0.00022	0.03	1.0	2.0

[a] Concentrations are in μEq L^{-1}, except for Si (μmol L^{-1}). SD = standard deviation; CV = coefficient of variation; SEF = sulfate equivalent fraction ($SO_4^{2-}/(SO_4^{2-}+HCO_3^{-})$); ND = no data.

ratios >0.70989, whereas the other four produced values <0.70906). The lower values are similar to those determined for dolomites (0.70901 ± 0.00055). The lowest calcite ratios (0.70845) overlap values appropriate for late Devonian seawater (Burke et al., 1982), whereas the highest calcite ratios approach 0.712, which is the value of the maximum strontium isotope ratio of basinal shale (MASIRBAS; Machel and Cavell, 1999). MASIRBAS is defined in terms of the carbonate fraction of Devonian age basinal shales from the Alberta Basin that is relatively easily leachable both in the laboratory and under near surface diagenetic conditions. The dolomite values are typical of Upper Devonian matrix dolomites from the Alberta Basin (0.7085 to 0.7095; Machel and Cavell, 1999).

The two different hydrochloric acid leaches produced $^{87}Sr/^{86}Sr$ ratios that are identical to within ± 0.00001 on all three samples analyzed. The carbonate $^{87}Sr/^{86}Sr$ values derived from HCl leaches and those derived from no. 1 acetic acid leaches differ by no more than ±0.00014, indicating that these three leach protocols are not significantly different in the Sr released to solution. The HCl (1) leaches give a mean carbonate ratio of 0.70978 ± 0.00081, which is distinctly higher than late Devonian seawater values. These results suggest that Sr in carbonates at Robertson Glacier consists of Devonian marine Sr mixed with small but variable amounts of more radiogenic Sr.

The $^{87}Sr/^{86}Sr$ ratio of ammonium acetate–exchangeable Sr from the till (0.71025) is higher than the mean calcite/dolomite values but significantly lower than the mean silicate value. It can be explained if around 0.77% of the exchangeable Sr is derived from weathering of silicate minerals with $^{87}Sr/^{86}Sr$ = 0.77098 (the mean value derived from the HF/HNO_3 leaches) and 99.23% from weathering of carbonates with $^{87}Sr/^{86}Sr$ = 0.70978 (the mean value from the HCl leaches). However, this calculation assumes either that the exchangeable Sr pool contains no atmospherically derived Sr or that this component has an isotopic ratio identical to either the carbonate- or silicate-derived components. Some previous studies have suggested that the exchangeable Sr in the surface layers of soils in alpine areas of western North America may contain a significant atmospheric component (Blum and Erel, 1997; Clow et al., 1997).

4.3. Major Ion Chemistry of Meltwaters

Table 4 summarizes the chemical characteristics of meltwater samples collected from the supraglacial stream and from the two meltwater streams draining Robertson Glacier. Except for Na and Cl, the concentrations of all species in the supraglacial stream are much lower than the mean concentrations in the meltwater streams. This suggests that most solute in the supraglacial stream is incorporated directly from snow or ice melt, whereas solute in the proglacial streams is derived predominantly from subglacial weathering. However, the concentrations of the dominant species in the supraglacial stream, Ca and HCO_3, are high enough to suggest that the supraglacial waters may have acquired a small amount of solute from dissolution of calcite dust on the glacier surface. The similarity of Na and Cl concentrations between the supraglacial and proglacial streams suggests that Na and Cl in proglacial runoff were derived mainly from snow and ice melt. However, in both streams, Na/Cl increases with total solute concentration (data not shown), indicating that the more concentrated proglacial samples at least may have acquired some Na from rock weathering at the glacier bed.

For both proglacial streams, the mean water composition is $Ca > HCO_3 > SO_4 > Mg \gg K$. However, there are some noticeable interstream differences. Excluding Na and Cl, the mean concentrations of all species except K are lower in RE than in RW. For all species except Sr, concentrations are also much more variable in RE (as expressed by the coefficient of variation).

Parameters indicating the likely provenance of solute also exhibit differences between the two streams. The equivalent ratio Ca/Mg is higher in RE than RW, indicating a higher proportion of solute derived from calcite relative to dolomite. K is also higher in RE than RW, indicating that weathering of K-silicates makes a greater contribution to the solute load of this stream. The sulfate equivalent fraction ($SO_4/(SO_4$ +

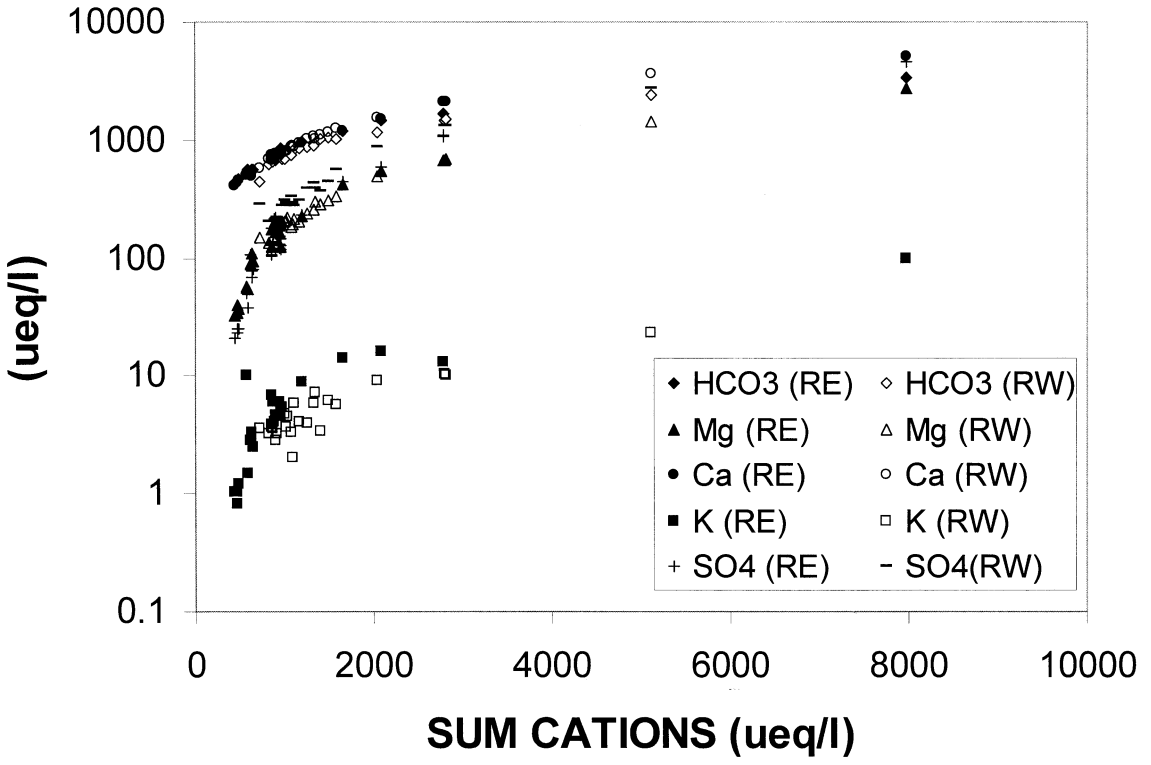

Fig. 1. The relationship between the concentration of individual ions (Ca^{2+}, Mg^{2+}, K^+, HCO_3^-, and SO_4^{2-}) and the total cation concentration in Robertson Glacier meltwaters (data from RE and RW displayed separately).

HCO_3)) serves as an indicator of the relative importance of carbonation and sulfide oxidation as sources of protons consumed in weathering reactions. The mean value of this parameter is higher in RW than in RE, indicating that sulfide oxidation is proportionally more important as a source of protons in waters draining via this stream. As with solute concentrations, parameters indicating solute provenance are more variable in RE than in RW. Mean $^{87}Sr/^{86}Sr$ ratios in both streams are similar to the mean carbonate value derived from HCl (1) leaches of powdered bedrock. The ratio in RE is, however, slightly higher and more variable than that in RW.

The chemical composition of the meltwaters clearly changes systematically with their ionic strength (as expressed by the total cation concentration; Fig. 1). Although there are differences of detail between the 2 streams, the general trends are similar. Ca and HCO_3 dominate the chemistry of the most dilute waters ($\Sigma^+ < 800$ μEq L^{-1}), whereas Mg and SO_4 become progressively more important as solute concentration increases. Although Mg concentrations are always less than those of Ca, the two values converge in the most concentrated waters. At $\Sigma^+ > 3000$ to 4000 μEq L^{-1}, $SO_4 \geq HCO_3$. These results can be interpreted by a simple solute provenance calculation based on the following assumptions:

(a) Given that X-ray diffraction does not show the presence of Ca/Mg-silicates in local bedrock, it is assumed that all Mg is derived from weathering of dolomite.

(b) Congruent dolomite weathering releases an amount of Ca equal (in equivalents) to the amount of Mg released.

(c) All remaining Ca is derived from weathering of calcite (this assumes zero contribution from alkali feldspar, which may contain up to 2% Ca).

(d) All K is derived from weathering of K-feldspar and/or muscovite. Cl concentrations in snow on Robertson Glacier average 0.82 ± 0.79 μEq L^{-1}, indicating that no correction for the sea salt contribution to K in runoff is necessary.

(e) All SO_4 is assumed to derive from sulfide oxidation. There are no known outcrops of evaporites in the catchment, and results of isotopic analyses on dissolved SO_4 support this assumption. Values of $\delta^{34}S$-SO_4 were -1.61 and 3.80 per mil. These are consistent with a sulfide source for SO_4 (Krouse, 1980), and much lower than values typically associated with Palaeozoic evaporites (Claypool et al., 1980). Values for $\delta^{18}O$-SO_4 were -13.68 and -14.50 per mil. Although values of $\delta^{18}O$-H_2O were not measured in this study, previously published values for this region fall in the range -17.5 to -20 per mil (Yonge et al., 1989). On a plot of $\delta^{18}O$-SO_4 vs. $\delta^{18}O$-H_2O, these samples would fall within the theoretical sulfide oxidation field of van Stempvoort and Krouse (1994).

(f) Acidity generated by sulfide oxidation is assumed to be neutralized by the weathering of carbonates, as a result of which an amount of HCO_3 equal (in equivalents) to the SO_4 concentration is released from bedrock. This is referred to as "rock HCO_3."

(g) The remaining bicarbonate is partitioned as follows: (1) an amount equal to the K concentration is derived from dissolution of CO_2 consumed in weathering K-silicates, and (2) the residual is assumed to be derived equally from carbonate bedrock (this fraction is added to the "rock HCO_3" pool) and from

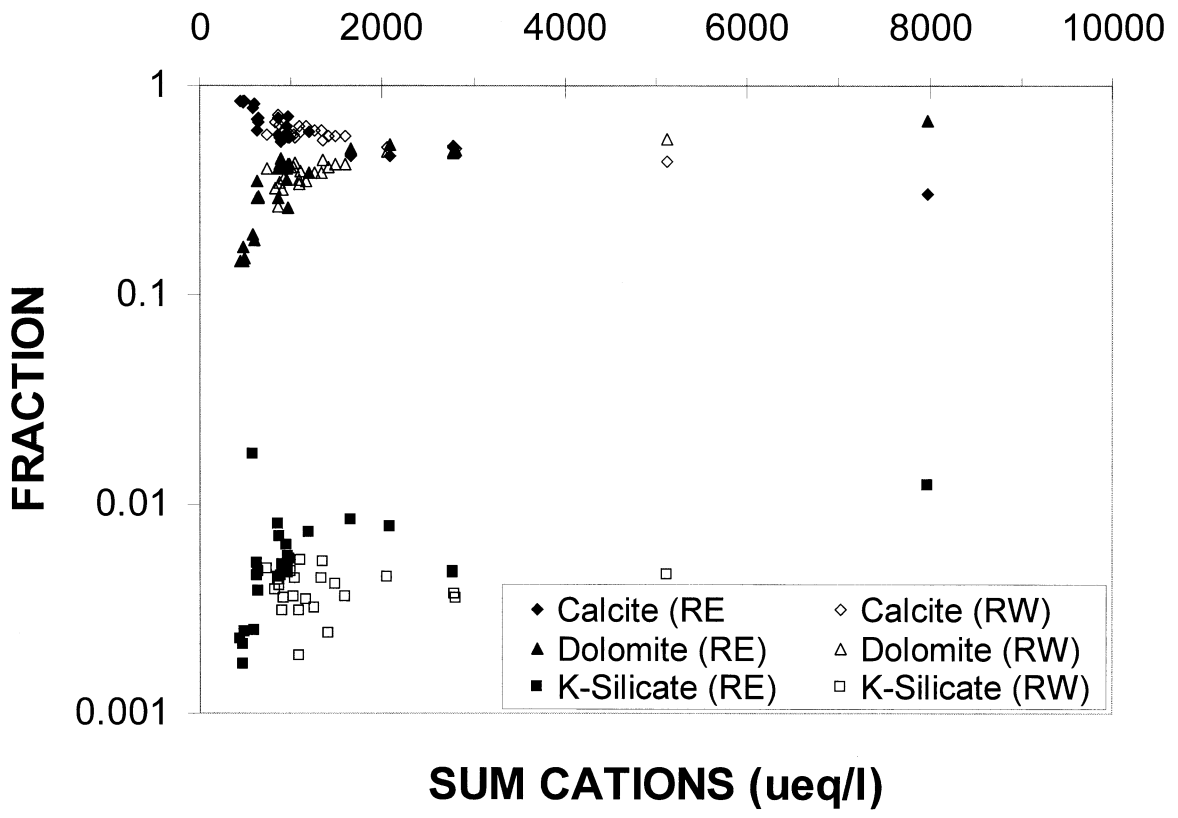

Fig. 2. Fraction of total cation load derived from dissolution of calcite, dolomite, and K-silicates as a function of total cation concentration in Robertson Glacier meltwaters (data from RE and RW displayed separately).

dissolution of CO_2 consumed in weathering calcite and dolomite. HCO_3 derived from CO_2 dissolution is referred to as "atmospheric HCO_3," although it is recognized that some of it could be derived from microbial oxidation of organic carbon.

As solute concentration increases, the dominant solute source changes from calcite to dolomite (Fig. 2). K concentration increases with total solute concentration (Fig. 1), but the proportion of cations derived from K-silicate weathering does not obviously increase in RW (Fig. 2). In RE, however, there is a suggestion that the proportional K-silicate contribution to the cation load increases up to total cation concentrations of $\sim$2500 μEq L^{-1} but remains constant beyond that point.

In the most dilute waters, HCO_3 is the dominant anion. It is derived almost equally from rock and atmospheric sources (Fig. 3), suggesting that CO_2 dissolution is the dominant proton source in these waters. As solute concentration increases, rock HCO_3 continues to increase, but SO_4 becomes more important than atmospheric HCO_3 at $\Sigma^- > 1500$ μEq L^{-1}, indicating that sulfide oxidation becomes the dominant proton source for the most concentrated waters. At $\Sigma^- > 4000$ μEq L^{-1}, SO_4 becomes the dominant anion and concentrations of atmospheric HCO_3 stabilize or even decrease. This behavior results from calcite precipitation driven by the common ion effect with dolomite dissolution, which is coupled to sulfide oxidation. Thus, the effects of de-dolomitization are recorded in the chemistry of these most concentrated waters.

The major ion chemistry of Robertson Glacier meltwaters indicates that solute acquisition is a staged process controlled by the relative dissolution kinetics of the major mineral phases present in local bedrock. The initial (rapid) stage of weathering involves acid hydrolysis of calcite, fueled by protons derived from dissolution of CO_2 in meltwaters and subsequent dissociation of H_2CO_3. The second stage involves acid hydrolysis of both calcite and dolomite, fueled increasingly by protons derived from sulfide oxidation. The final stage involves sulfide oxidation-driven acid hydrolysis of dolomite, accompanied by calcite precipitation. K-silicate weathering and perhaps ion exchange also occur (particularly in RE), but their place in the sequence of weathering reactions is less clear.

The mean compositions of meltwaters sampled from RE and RW indicate that rapid initial weathering reactions have the most influence on the chemistry of relatively dilute RE waters, whereas second and final stage reactions are more important for the chemistry of the more of concentrated RW waters. The high degree of variability in the chemistry of RE waters is consistent with the observation that RE shows a more flashy hydrological response to summer diurnal melt cycles than RW. At peak daily discharges, RE waters are dilute and the effects of rapid weathering reactions dominate their chemistry, whereas at daily minimum flow they are more concentrated and their chemistry is influenced by second and final stage reactions. By contrast, meltwater discharge in RW does not vary greatly and dolomite dissolution and sulfide oxidation are always more important influences on the meltwater chemistry.

The observed differences in the chemical characteristics of RE and RW meltwaters suggest differences in the characteris-

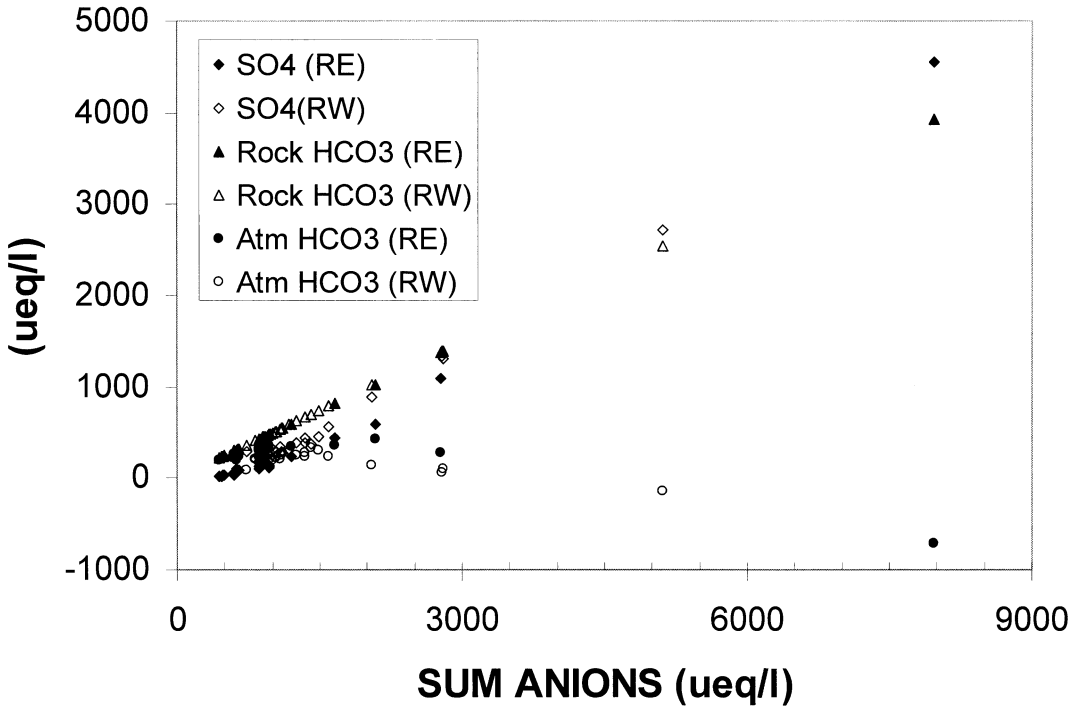

Fig. 3. Provenance of anions in Robertson Glacier meltwaters as a function of the total anion concentration (data from RE and RW displayed separately). See text for method of calculation.

tics of the subglacial drainage systems feeding the two streams. The difference in mean solute concentration suggests that waters draining via RE have a lower mean subglacial residence time than those draining via RW. The higher variability in concentration/composition in RE suggests that this stream is fed by a more complex drainage system than RW. Such a drainage system must include elements with different mean subglacial residence times. At peak flows, runoff is dilute and the products of rapid reactions (e.g., calcite dissolution) dominate the solute load. This suggests that most water draining through RE under these conditions has passed rapidly through the glacier, probably via a system of major subglacial channels (e.g., Röthlisberger, 1972). At low flows, runoff is more concentrated and much of the solute load is derived from reactions that take place more slowly (e.g., dolomite dissolution and sulfide oxidation). This suggests that waters draining through RE under these conditions have spent some time in a qualitatively different hydrological/weathering environment, such as a distributed subglacial drainage system. Possible components of such a system include subglacial cavities and Nye channels (cf. Walder and Hallet, 1979), a thin subglacial water film (from which the observed subglacial calcites are likely to have precipitated; Hallet, 1976), and/or the pore space of subglacial tills. The high mean solute concentration and solute composition in RW, together with their low variability, suggest that a distributed system supplies the bulk of runoff to this stream at all times.

4.4. Strontium Isotopes in Meltwaters

The concentration of Sr in both streams increases with solute concentration (Fig. 4), but at higher solute concentrations the increase in RW appears to be logarithmic, whereas that in RE is linear and more gradual. $^{87}Sr/^{86}Sr$ ratios from RW waters lie consistently close to the mean values produced by leaching bedrock powders with hydrochloric acid (0. 70938 −0.70978) (Fig. 5). The highest value of $^{87}Sr/^{86}Sr$ recorded in RE waters (0.71058) exceeds that determined for the exchangeable Sr pool in till, whereas the lowest value (0.709337) lies between the mean values determined for calcite and dolomite. In RW, $^{87}Sr/^{86}Sr$ shows no systematic variation with the concentration of total cations, K, or Sr (Figs. 5 to 7), whereas in RE it increases logarithmically with each of these variables. This is consistent with the greater variability in chemical composition of RE meltwaters discussed above.

Together, these results suggest that the variability in $^{87}Sr/^{86}Sr$ in waters from RW could be attributable entirely to the variability in the isotopic composition of carbonate minerals in the catchment and that all of the Sr dissolved in these waters could be derived from carbonate sources. The range of isotopic compositions recorded in waters from RE also lies within that found in hydrochloric and acetic acid leaches of bedrock samples. However, the observation that $^{87}Sr/^{86}Sr$ increases systematically with the concentrations of cations, Sr and K strongly suggests a systematic change in the balance of Sr sources as weathering progresses. Because the $^{87}Sr/^{86}Sr$ ratio of HF/HNO_3 leaches of bedrock is considerably higher than that of leaches designed to extract carbonate minerals (Table 3), it is probable that these trends reflect an increasing influence of Sr from K-silicate dissolution on $^{87}Sr/^{86}Sr$ of the more concentrated waters from RE. The inverse relationship between $^{87}Sr/^{86}Sr$ and the ratio Ca/K for waters from RE (Fig. 8) provides

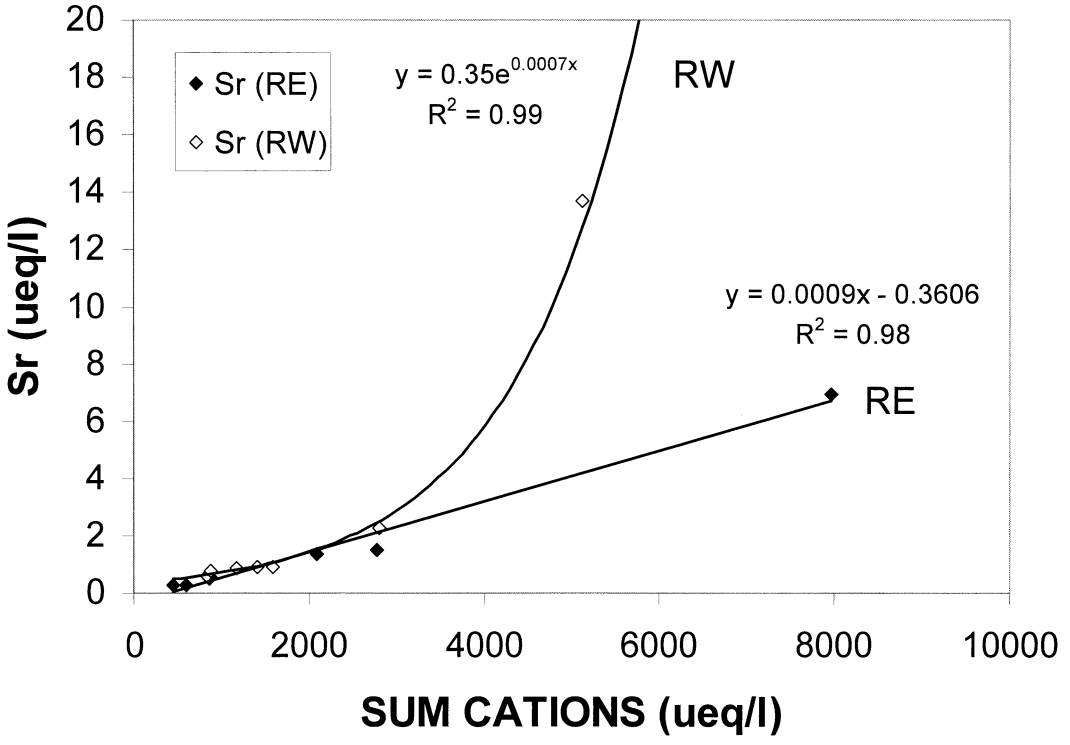

Fig. 4. Relationship between the concentration of Sr^{2+} and total cation concentration in Robertson Glacier meltwaters (data from RE and RW displayed separately). Linear, logarithmic, exponential, and power law regressions were computed for each data set, and the regression that yielded the highest r^2 value is displayed.

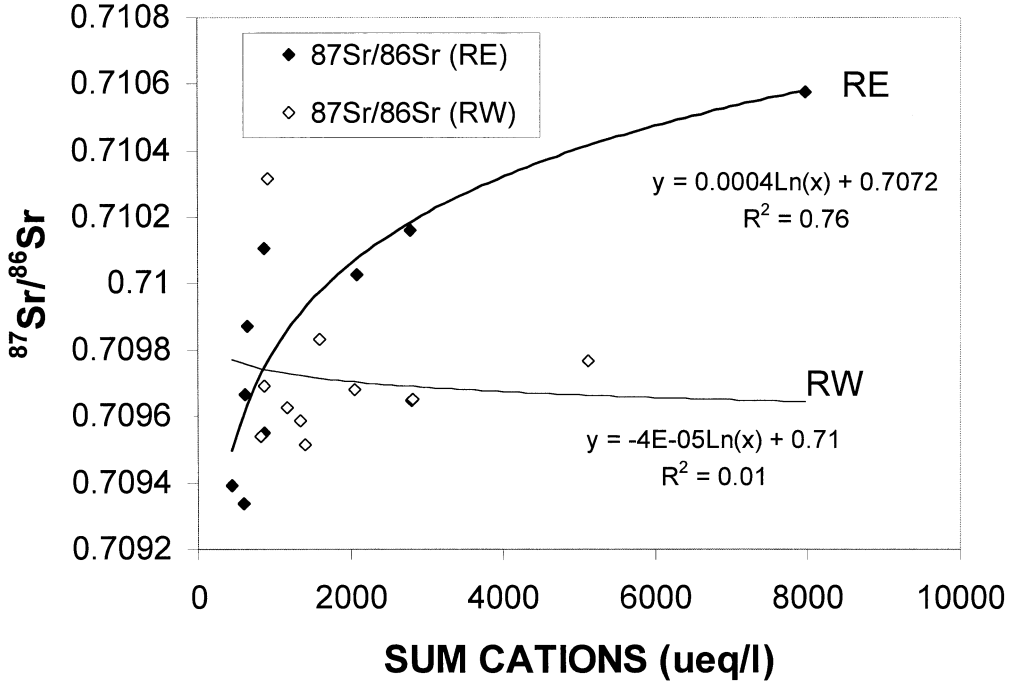

Fig. 5. Relationship between $^{87}Sr/^{86}Sr$ and total cation concentration in Robertson Glacier meltwaters. Linear, logarithmic, exponential, and power law regressions were computed for each data set (RE and RW), and the regression that yielded the highest r^2 value is displayed.

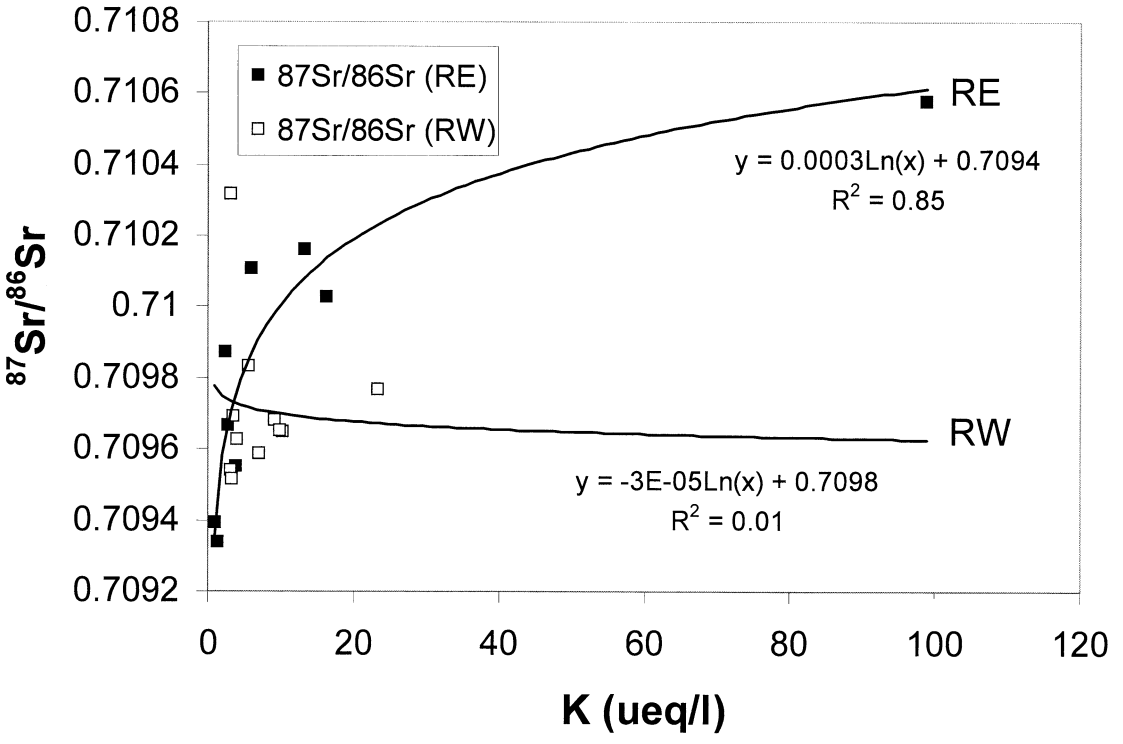

Fig. 6. Relationship between $^{87}Sr/^{86}Sr$ and K concentration in Robertson Glacier meltwaters. Linear, logarithmic, exponential, and power law regressions were computed for each data set (RE and RW), and the regression that yielded the highest r^2 value is displayed.

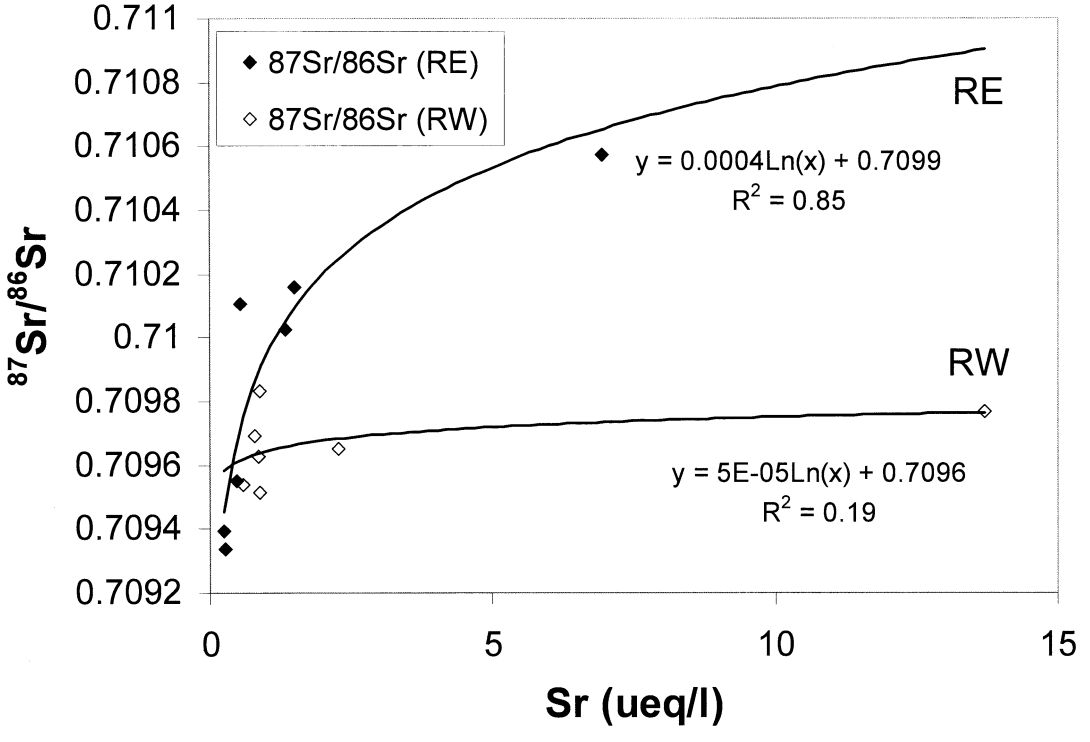

Fig. 7. Relationship between $^{87}Sr/^{86}Sr$ and Sr concentration in Robertson Glacier meltwaters (data from RE and RW displayed separately). Linear, logarithmic, exponential, and power law regressions were computed for each data set, and the regression that yielded the highest r^2 value is displayed.

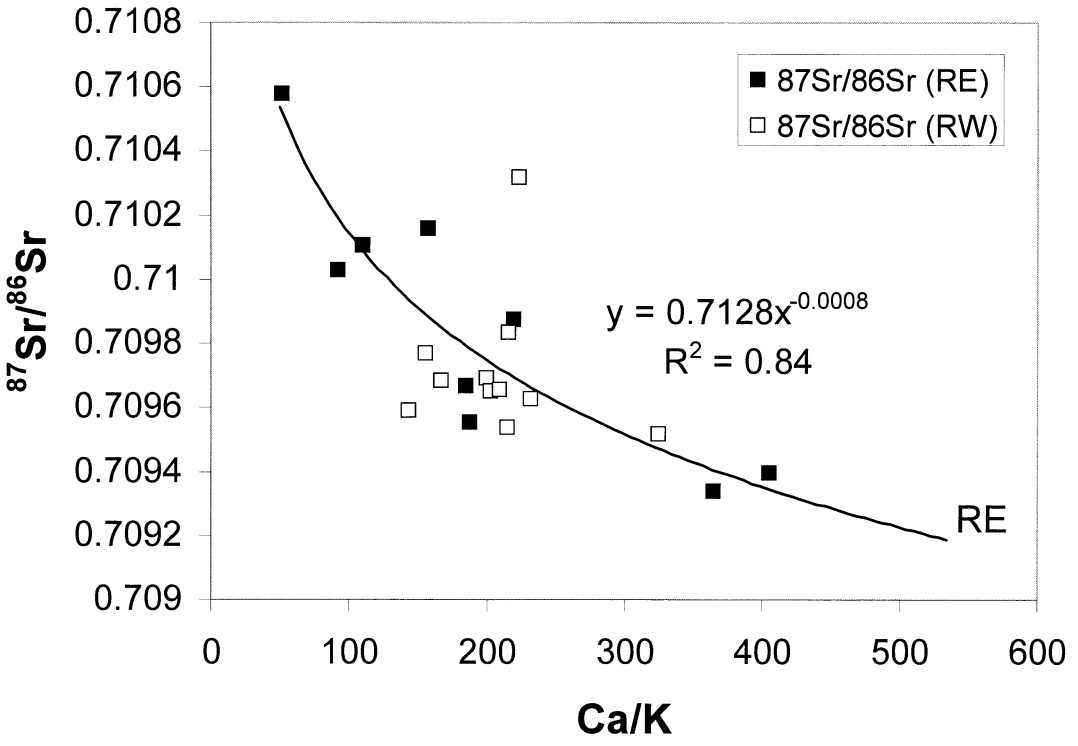

Fig. 8. Relationship between $^{87}Sr/^{86}Sr$ and the ratio (Ca/K) in Robertson Glacier meltwaters (data from RE and RW displayed separately). Linear, logarithmic, exponential, and power law regressions were computed for each data set (RE and RW), and the regression that yielded the highest r^2 value for RE is displayed.

further support for this suggestion, which is discussed in more detail below.

The tendency for $^{87}Sr/^{86}Sr$ in RE to increase with Sr concentration is the opposite of the trend displayed by data sets for both global (Palmer and Edmond, 1989) and Himalayan rivers (Galy et al. 1999). The global trend is defined by mixing of Sr derived from weathering of limestones and evaporites with Sr derived from weathering of silicate rocks. Limestones and evaporites contain high concentrations of Sr with low $^{87}Sr/^{86}Sr$ and are assumed to be the dominant source of Sr in more concentrated waters. Relative to carbonate rocks, silicate rocks typically contain lower concentrations of Sr with high $^{87}Sr/^{86}Sr$, and they are assumed to be the dominant source of Sr in dilute waters. In RE waters, however, carbonate weathering is the dominant solute source at all solute concentrations and the amount of Sr derived from carbonate dissolution must be higher in the more concentrated waters. The increase in $^{87}Sr/^{86}Sr$ with solute and Sr concentration in these waters is therefore likely to reflect either an increased proportional contribution of Sr from K-silicate weathering in more concentrated waters or a shift in the isotopic composition of K-silicate-derived Sr between the more dilute and more concentrated waters. Clow et al. (1997) reported a similar change in Sr sources, from calcite to K-silicates, with progressive leaching of crushed gneiss from the Loch Vale watershed, Colorado.

Four processes could produce the relationships observed: changes in the relative dissolution rates of carbonate and K-silicate minerals, preferential release of Sr over K from freshly ground silicate surfaces, nonstoichiometric release of $^{87}Sr/^{86}Sr$ during K-silicate weathering, and a change in the relative amounts of Sr derived from different K-silicate minerals. These are now discussed in detail.

4.4.1. *Changes in the Relative Dissolution Rates of Carbonate and K-Silicate Minerals*

If K-silicate–derived Sr is released by stoichiometric dissolution of a single K-silicate phase, the observations could be explained if the rate of K-silicate dissolution increased relative to that of carbonate dissolution as waters became more concentrated. This might occur if the supply of carbonate minerals became exhausted by progressive weathering (Clow et al., 1997), but this seems highly unlikely in this predominantly carbonate catchment. Alternatively, rates of carbonate dissolution might slow as waters approach saturation with respect to calcite and dolomite. Regression analysis confirms that the saturation indices for both calcite and dolomite increase with solute concentration. The trends are weak but statistically significant ($SI_{calcite} = 0.437 \text{ Ln } \Sigma^+ - 3.6$, $r^2 = 0.27$; $SI_{dolomite} = 1.121 \text{ Ln } \Sigma^+ - 9.8$, $r^2 = 0.36$).

If it is assumed that the Sr isotopic composition of meltwaters is attributable entirely to variable mixing of Sr derived from stoichiometric dissolution of carbonates and a single K-silicate phase, the implied variation in the fraction of Sr derived from K-silicate weathering can be estimated by a mass balance calculation:

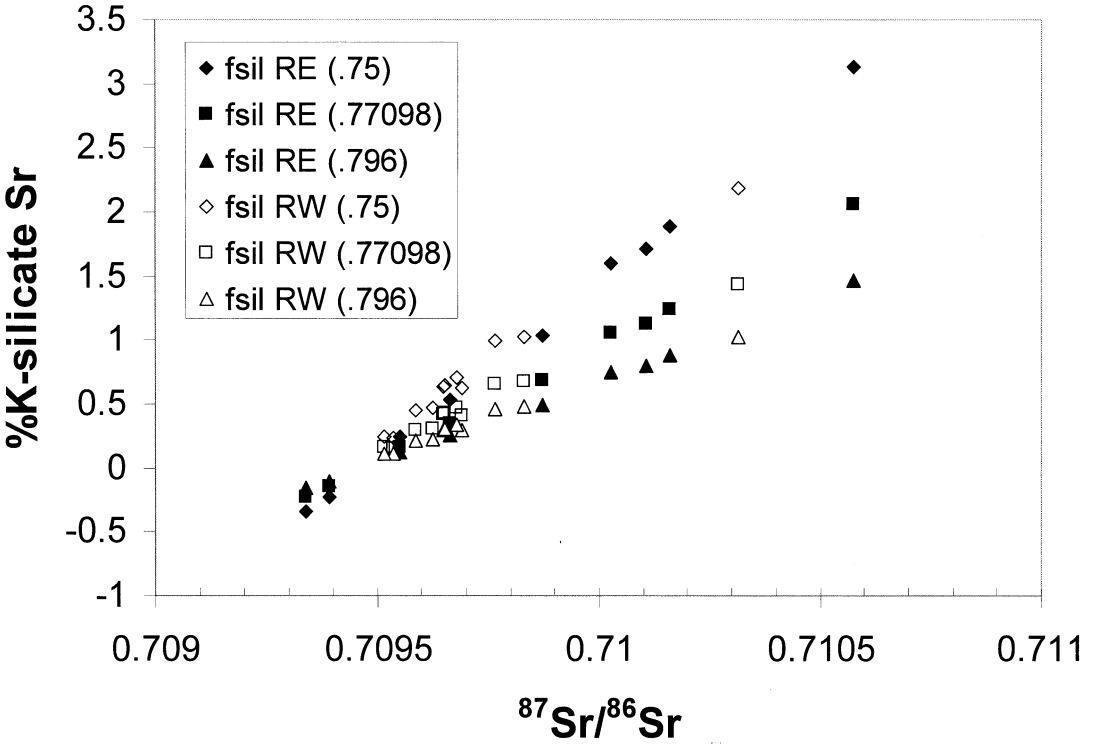

Fig. 9. Relationship between $^{87}Sr/^{86}Sr$ and the estimated proportion of Sr derived from weathering of K-silicate minerals in Robertson Glacier meltwaters. Symbols are keyed according to the stream from which samples were collected and the value of $^{87}Sr/^{86}Sr$ assumed for the K-silicate–derived fraction of strontium.

$$f\,(Sr_{K\text{-silicate}}) = (^{87}Sr/^{86}Sr_{water} - {}^{87}Sr/^{86}Sr_{carbonate})/ (^{87}Sr/^{86}Sr_{K\text{-silicate}} - {}^{87}Sr/^{86}Sr_{carbonate}), \quad (1)$$

where f ($Sr_{K\text{-silicate}}$) refers to the fraction of Sr in a sample derived from dissolution of the K-silicate phase, and the other terms refer to the isotopic composition of Sr in either a water sample or a specific mineral phase. To calculate the K-silicate–derived fraction of Sr in each sample, the isotopic composition of Sr derived from carbonate dissolution was first estimated:

$$^{87}Sr/^{86}Sr_{carbonate} = (^{87}Sr/^{86}Sr_{calcite} \times f\,(Sr_{calcite})) + (^{87}Sr/^{86}Sr_{dolomite} \times f\,(Sr_{dolomite})). \quad (2)$$

In this case, f refers to the fraction of carbonate-derived Sr produced by dissolution of either calcite or dolomite. These quantities were calculated on the assumption that solute derived from carbonate weathering had a Sr:Ca ratio identical to that of the source mineral (which may be unlikely because Ca is often preferred over Sr in the calcite lattice, resulting in Sr/Ca being higher in weathering solutions than in the solid phase; English et al., 2000). Molar Sr:Ca ratios of the bedrock samples with the highest and lowest calcium contents respectively were used as estimates of the ratio in calcite (0.0005) and dolomite (0.00032). The amounts of Ca released from calcite and dolomite dissolution were estimated by assuming that dolomite weathering released an amount of Ca equal to the amount of Mg in a sample, and that the remaining Ca in a sample came from calcite dissolution. The calculation used mean values of $^{87}Sr/^{86}Sr$ for calcite and dolomite derived from acetic acid leaching of bedrock powders (Table 3).

In cases where $^{87}Sr/^{86}Sr_{carbonate}$ is higher than the measured sample value, Eqn. 1 calculates a negative contribution from K-silicate sources. This is taken to imply that all Sr in these samples was derived from carbonate weathering. For other cases, the contribution of Sr from K-silicate weathering was estimated by Eqn. 1 for three different scenarios. The first assumed that K-silicate-derived Sr had $^{87}Sr/^{86}Sr$ equal to the mean value derived from HF/HNO_3 dissolution of bedrock powders (0.77098; Table 3). The other two cases assumed K-silicate Sr with $^{87}Sr/^{86}Sr$ ratios of 0.75 (leach of R1, in which K-feldspar was the only K-silicate detected by X-ray diffraction) or 0.796 (leach of R5 in which muscovite was the only K-silicate detected). The validity of the assumption of stoichiometric release of $^{87}Sr/^{86}Sr$ during K-silicate weathering is discussed further below.

The results (Fig. 9) show that for both RE and RW there is a strong linear relationship between $^{87}Sr/^{86}Sr$ and the proportion of Sr derived from K-silicate sources. This proportion ranges from less than 0% in the two least radiogenic samples to more than 3% in the most radiogenic sample if $^{87}Sr/^{86}Sr$ of K-silicate Sr is 0.75. The two most dilute samples contain no K-silicate–derived Sr, regardless of what assumptions are made about the isotopic composition of this Sr. As expected from the major ion chemistry, waters from RE require a greater input of K-silicate–derived Sr than those from RW. The mean contributions required range from 0.5 ± 0.53% ($^{87}Sr/^{86}Sr$ of

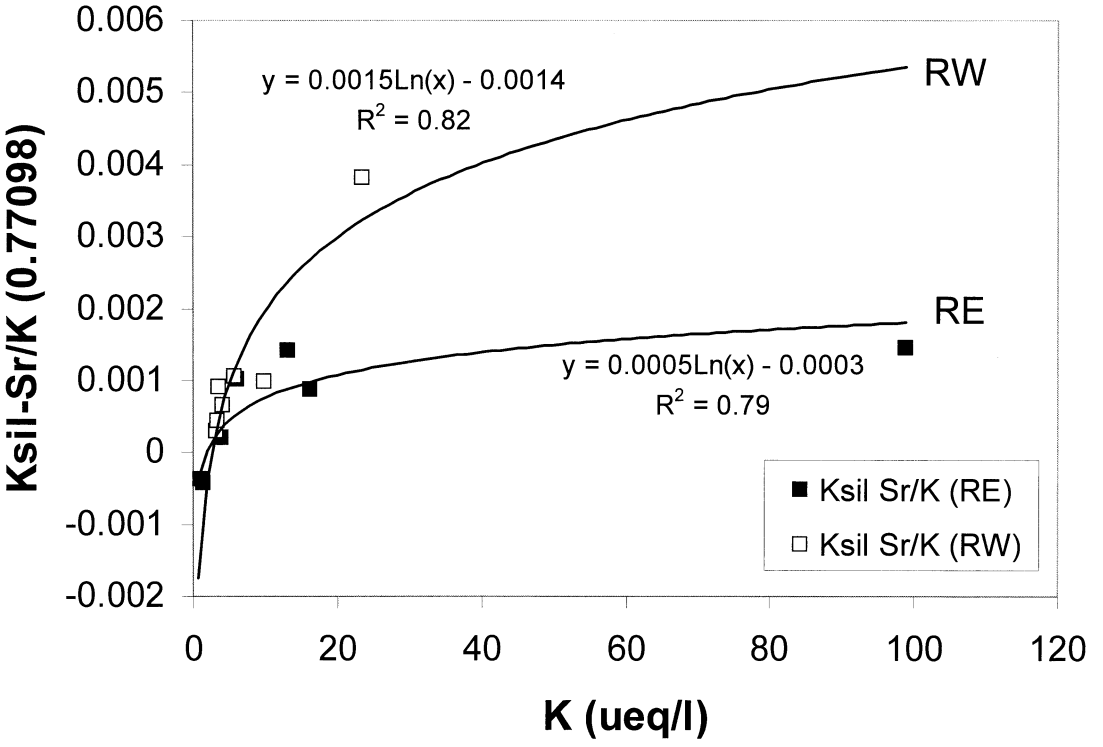

Fig. 10. Relationship between the ratio (K-silicate Sr/K) and K in Robertson Glacier meltwaters (data from RE and RW displayed separately). K-silicate Sr was calculated on the assumption that it had $^{87}Sr/^{86}Sr = 0.77098$. Linear, logarithmic, exponential, and power law regressions were computed for each data set (RE and RW), and the regression that yielded the highest r^2 value is displayed.

K-silicate Sr = 0.796) to 1.06 ± 1.13% ($^{87}Sr/^{86}Sr$ of K-silicate Sr = 0.75) of the total Sr for RE, and 0.35 ± 0.25% (0.796) to 0.75 ± 0.54% (0.75) for RW.

Although only a single sample from RW has $^{87}Sr/^{86}Sr$ more than 0.71000 and requires more than 1% K-silicate Sr in any of the scenarios, four samples from RE have these characteristics. As noted above, the $^{87}Sr/^{86}Sr$ ratios, and lack of relationships between $^{87}Sr/^{86}Sr$ and total cations, Sr and K in samples from RW may be indicative of a carbonate source for Sr in these samples (except perhaps for the single sample with $^{87}Sr/^{86}Sr >$ 0.71000). If so, it follows that those samples from RE with $^{87}Sr/^{86}Sr$ less than 0.71000 could also contain Sr derived exclusively from carbonate sources. In this case, only the 4 most concentrated samples from RE carry a Sr isotopic fingerprint of K-silicate dissolution. This interpretation may, however, be excessively conservative given the strength of the relationships between $^{87}Sr/^{86}Sr$ and total cations, Sr, K, and Ca/K in samples from RE.

4.4.2. Preferential Release of Sr over K from Freshly Ground Silicate Surfaces

Under acid conditions in the laboratory, initial leaching of cations from newly abraded silicate surfaces occurs upon solution equilibration (Blum and Stillings, 1995; Stillings and Brantley, 1995). This results in high initial Sr release rates (Taylor et al., 2000a,b). When waters are far from equilibrium with the mineral surface, dissolution may occur primarily by etch pit formation at defect sites where Sr can be concentrated (Taylor et al., 2000a). Sr may then be released preferentially over K. At the glacier bed, such conditions may be replicated where dilute meltwaters first come into contact with freshly ground bedrock, or where sulfide oxidation takes place and sulfuric acid is produced. This is most likely in areas of the bed characterized by distributed subglacial drainage, where ice is in intimate contact with subglacial sediments and crushing and abrasion are active. It is less likely in major subglacial channels, where dilute waters acquire much of their solute from suspended sediment particles with surfaces that may have been depleted in cations during a previous phase of weathering (Brown et al., 1994). Such surfaces are likely to have equilibrated with the meltwaters and to dissolve stoichiometrically (Brantley et al., 1998). This could explain the enhanced K-silicate contribution to the Sr load of the more concentrated meltwaters that are derived primarily from a distributed subglacial drainage system.

To test this hypothesis, the amount of K-silicate–derived Sr in each sample was estimated by measurements of Sr concentration and the estimate of the K-silicate–derived fraction of Sr for $^{87}Sr/^{86}Sr = 0.77098$ (the amounts estimated would obviously vary depending upon the value of $^{87}Sr/^{86}Sr$ assumed). The ratio K-silicate Sr/K was then calculated for each sample. If the initial assumption of stoichiometric dissolution of a single K-silicate phase is correct, then this ratio should be independent of K concentration. In fact, it increases logarithmically with K in both meltwater streams (Fig. 10). This result

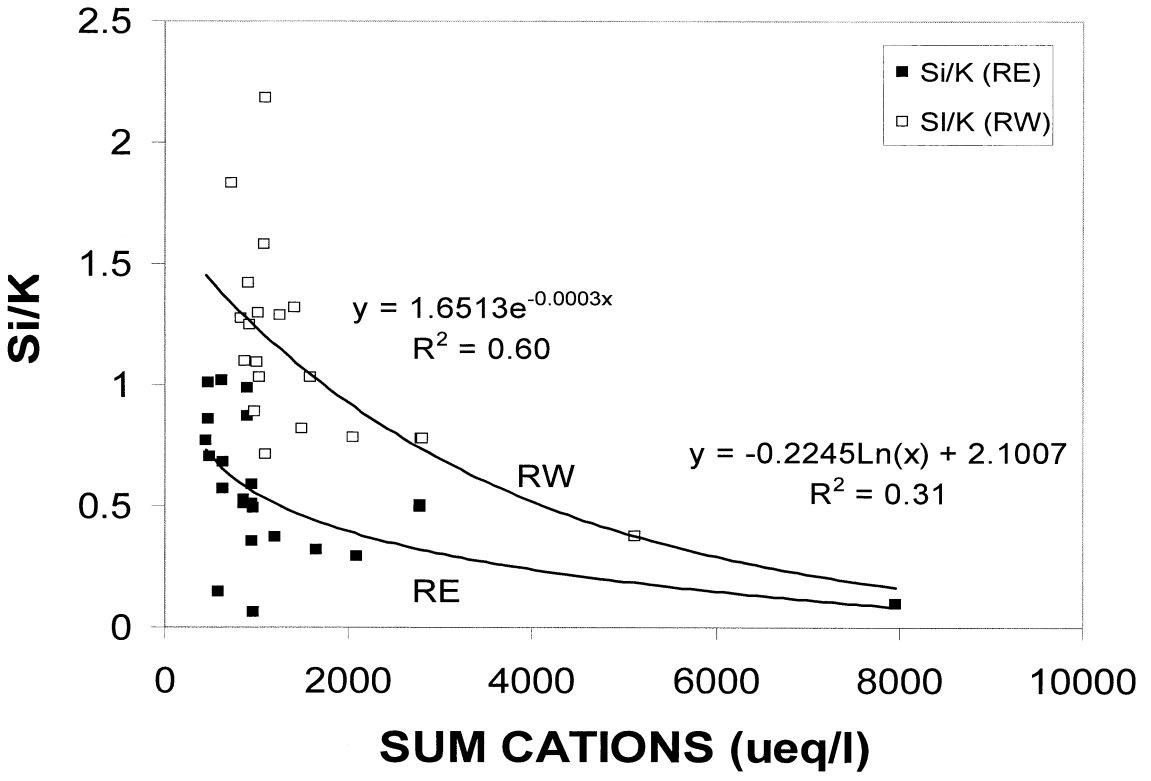

Fig. 11. Relationship between the ratio (Si/K) and total cation concentration in Robertson Glacier meltwaters (data from RE and RW displayed separately). Linear, logarithmic, exponential, and power law regressions were computed for each data set, and the regression that yielded the highest r^2 value is displayed.

is at least consistent with the hypothesis that Sr is released preferentially over K under conditions that generate the most concentrated runoff. However, as will be discussed below, there are alternative interpretations.

4.4.3. *Nonstoichiometric Release of $^{87}Sr/^{86}Sr$ during K-Silicate Weathering*

Thus far, it has been assumed that $^{87}Sr/^{86}Sr$ of Sr released during K-silicate weathering is identical to that of Sr in the bulk source mineral. However, laboratory experiments suggest that this is often not the case (Brantley et al., 1998; Taylor et al., 2000b). Radiogenic ^{87}Sr, which is produced by the radioactive decay of ^{87}Rb, is a trace constituent in K-silicate minerals. It may therefore reside in sites that are especially susceptible to preferential reaction with weathering solutions (such as dislocations, strained regions and other defect sites with excess energy; Bullen et al., 1997). As a result, it may be released preferentially over ^{86}Sr during initial dissolution of certain minerals (e.g., bytownite, Brantley et al., 1998; biotite and phlogopite, Taylor et al., 2000b). Furthermore, some K-silicate minerals contain trace phases (such as zeolites, calcite, apatite and albite) that can have a very different $^{87}Sr/^{86}Sr$ to the primary mineral (Brantley et al., 1998; Taylor et al., 2000b). If these trace phases initially dissolve more rapidly than the primary mineral, but become exhausted as dissolution progresses, then $^{87}Sr/^{86}Sr$ of the solution will change over time. It can either decrease or increase, depending on whether Sr in the secondary phase is more or less radiogenic than Sr in the primary mineral.

It is therefore possible that the $^{87}Sr/^{86}Sr$ values derived from the HF/HNO_3 leaches do not provide a reliable guide to the isotopic composition of Sr released by K-silicate weathering. The observed relationship between $^{87}Sr/^{86}Sr$ and Σ^+, Sr, and K in RE waters could be explained if weathering of a given K-silicate mineral in the distributed subglacial drainage system produced higher $^{87}Sr/^{86}Sr$ values than weathering of the same mineral in the channelized subglacial system. Because laboratory experiments indicate that $^{87}Sr/^{86}Sr$ of weathering solutions can be either higher or lower than that of the mineral being weathered and that this relationship may change over time (Brantley et al., 1998; Taylor et al., 2000b), it is not possible to quantify this effect.

Nevertheless, $^{87}Sr/^{86}Sr$ of Sr released during weathering of microcline (which is present in bedrock at Robertson Glacier) increased over time during dissolution experiments (Brantley et al., 1998). Thus, Sr released when microcline is weathered in environments that are characterized by long water:rock contact times (the distributed drainage system) may be more radiogenic than that released when it is weathered in environments with short rock:water contact times (the channelized drainage system). If so, then the variability in the Sr isotope composition of runoff may reflect residence-time-related variability in the difference between $^{87}Sr/^{86}Sr$ of microcline and of the Sr released when it is dissolved.

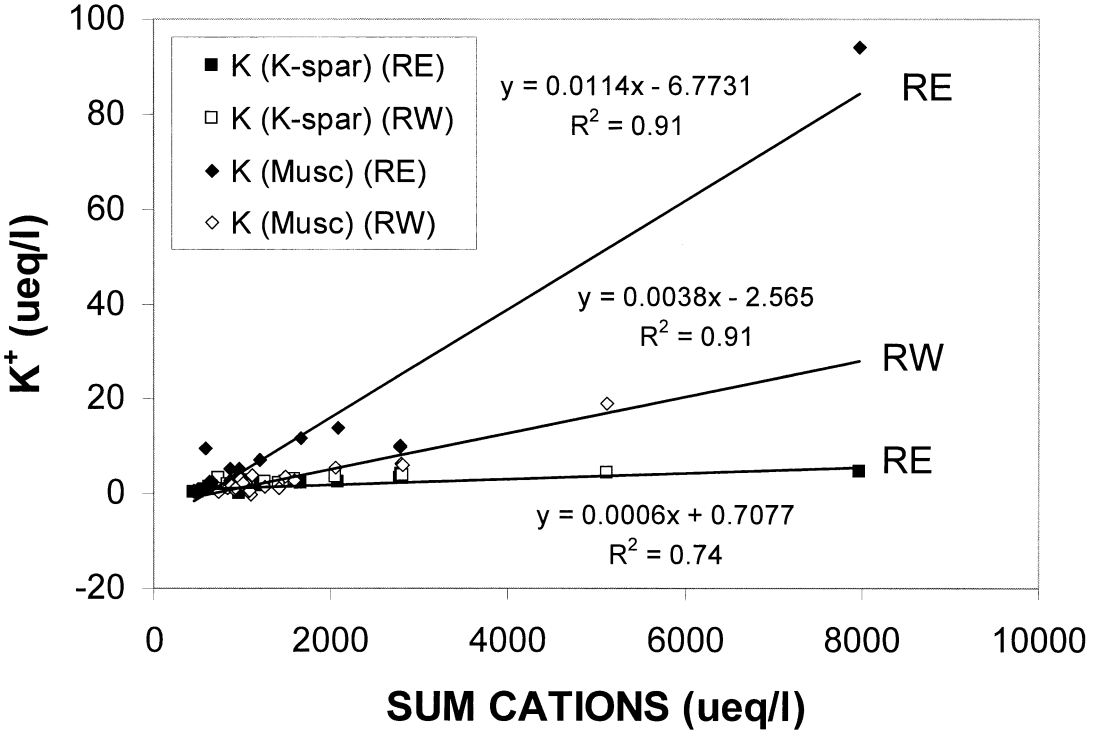

Fig. 12. K^+ concentrations in Robertson Glacier meltwaters attributable to dissolution of K-feldspar and muscovite in relation to total cation concentration (data from RE and RW displayed separately). Linear, logarithmic, exponential, and power law regressions were computed for each data set, and the regression that yielded the highest r^2 value is displayed.

4.4.4. *Change in the Relative Amounts of Sr Derived from Different K-Silicate Minerals*

The silicate-derived $^{87}Sr/^{86}Sr$ of muscovite-bearing sample R5 is substantially higher than that of samples R1 and R18, which, according to X-ray diffraction, contain only K-feldspars (Table 3). If, as this suggests, the $^{87}Sr/^{86}Sr$ of muscovite is higher than that of K-feldspar, then the apparent increase in the K-silicate contribution to Sr in more concentrated runoff could simply reflect a proportionally greater contribution from muscovite relative to K-feldspar.

The potential impact of such a change in Sr source on the K-silicate-derived fraction of Sr can be gauged from Figure 9. Calculations of the K-silicate contribution to Sr were performed for values of $^{87}Sr/^{86}Sr$ derived from HF/HNO_3 leaches of bedrock samples that X ray diffraction indicated contained only K-feldspar (R1, $^{87}Sr/^{86}Sr = 0.75$) or muscovite (R5, $^{87}Sr/^{86}Sr = 0.796$). For the most radiogenic sample analyzed, the K-silicate contribution to Sr ranges from 1.47% for an inferred muscovite source to 3.13% for an inferred K-feldspar source. The results clearly suggest that the K-silicate contribution to total Sr must increase as $^{87}Sr/^{86}Sr$ increases, even if the change in $^{87}Sr/^{86}Sr$ is also associated with a shift in Sr source from K-feldspar to muscovite. However, a note of caution is appropriate. Although muscovite was the only K-silicate detected in R5, $^{87}Sr/^{86}Sr$ of this sample is rather low for muscovite (Probst et al., 2000). The value may thus reflect a mixture of muscovite and another undetected mineral containing less radiogenic strontium. If this is the case, and $^{87}Sr/^{86}Sr$ of muscovite is significantly higher than has been assumed, the K-silicate contribution to Sr would be much lower than the estimates shown on Figure 9 for cases where muscovite is a major source of Sr.

The hypothesis that a shift in the relative importance of muscovite and K-feldspars as Sr sources is responsible for the radiogenic nature of the Sr found in the more concentrated RE waters can be evaluated by a plot of Si/K against total cations (Fig. 11). A value of $Si/K = 0$ is expected for weathering of muscovite to kaolinite, as all Al and Si are taken up in the clay product. A value of 2 is expected for weathering of K-feldspar to kaolinite, as one Al is matched by one Si in the clay, leaving 2 Si to 1 K in solution. With one exception, measured values of Si/K fall between 0 and 2, but they are consistently higher for RW (1.14 ± 0.42), than for RE (0.55 ± 0.27). This suggests that K-feldspar weathering is more important as a solute source for RW, whereas muscovite is more important for RE (Fig. 11). In both streams, however, Si/K decreases as solute concentration increases, indicating that muscovite dissolution becomes progressively more important at higher solute concentrations (Fig. 11). The range of Si/K values also decreases as solute concentration increases, implying that in the more concentrated waters K-silicate weathering is dominated by muscovite, whereas at lower concentrations the relative importance of muscovite and K-feldspar dissolution is quite variable (Fig. 11). This may reflect the short subglacial residence time of

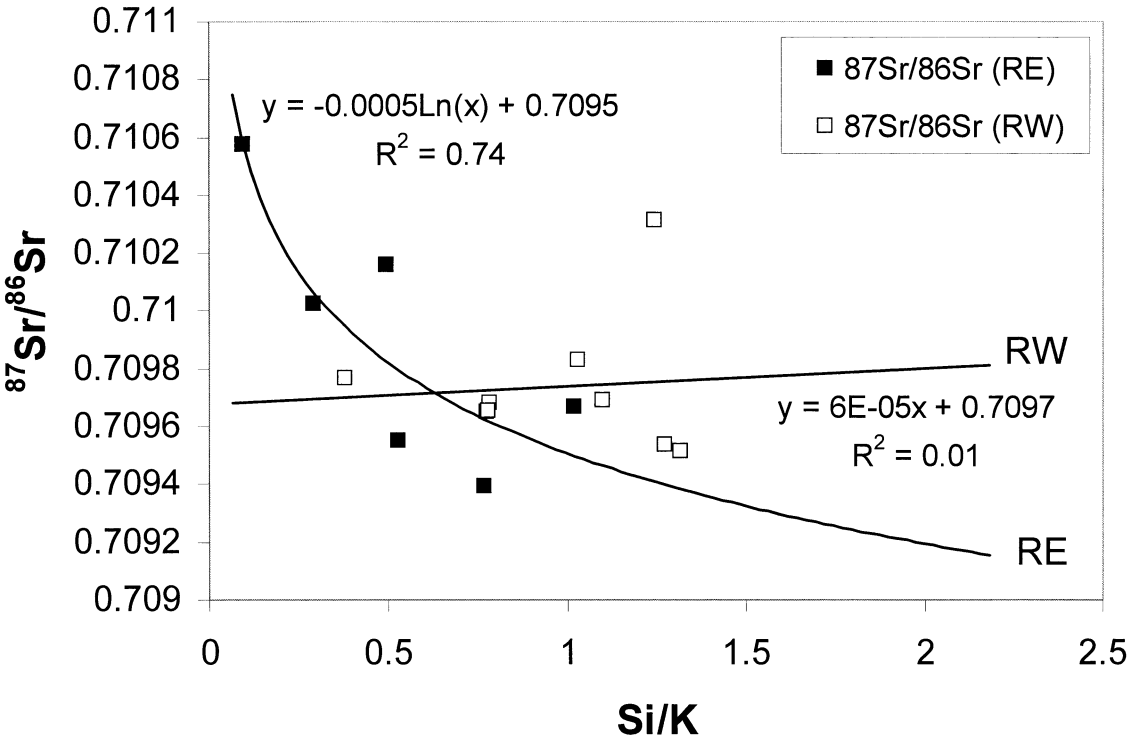

Fig. 13. $^{87}Sr/^{86}Sr$ in Robertson Glacier meltwaters as a function of the ratio (Si/K) (data from RE and RW displayed separately). Linear, logarithmic, exponential, and power law regressions were computed for each data set, and the regression that yielded the highest r^2 value is displayed.

dilute waters, which precludes homogenization of diverse water chemistries developed in different parts of the subglacial drainage system.

To quantify this discussion, the amount of K in each sample from dissolution of K-feldspar was estimated as (Si/2 μmol L^{-1}), and the amount from muscovite dissolution as (K − (Si/2) μmol L^{-1}) (Fig. 12). This assumes that both minerals weather to kaolinite. The contribution of K from K-feldspar is always very small in both streams. Linear regression with cation concentration gives a slope of 0.0006 in both streams. At total cation concentrations of less than 1000 μEq L^{-1}, the muscovite contribution is comparable in both streams, and similar to that from K-feldspar. However, it increases much more rapidly with cation concentration, especially in RE (linear regression slope of 0.0114 compared with 0.0038 in RW). Thus, muscovite is the dominant source of K in RE at cation concentrations of more than ~600 μEq L^{-1}. In RW, it only becomes dominant at cation concentrations of more than ~1200 μEq L^{-1}. Catchment geology may explain why muscovite dissolution is a more important source of K for RE than for RW. The Sassenach Formation, which consists of interbedded quartzose siltstones and sandstones, dark shales, argillaceous and silty limestones, outcrops in the catchment of RE (McMechan, 1988). These lithologies likely constitute a source of muscovite that is absent from the RW catchment.

In RW, there is no obvious association between $^{87}Sr/^{86}Sr$ and Si/K (Fig. 13). This is consistent with the suggestion made earlier that Sr inputs to RW waters are dominated by carbonate sources, and suggests that K-feldspar and muscovite weathering release insufficient Sr to have a discernible influence on $^{87}Sr/^{86}Sr$ in this stream. Although muscovite dissolution releases K to RW waters about an order of magnitude faster than K-feldspar dissolution (Fig. 12), the Sr content of muscovite is typically less than 30 ppm (Albuquerque, 1975), compared with a few hundred parts per million in K-feldspar (Smith, 1974, p. 38). The amounts of Sr released from the two sources are therefore comparable and small, which likely explains why muscovite dissolution has no discernible impact on $^{87}Sr/^{86}Sr$ of RW waters.

In RE, $^{87}Sr/^{86}Sr$ decreases logarithmically as Si/K increases (Fig. 13). Thus, the most radiogenic waters are those in which muscovite dissolution makes the dominant contribution to the K load. In RE, the rate of K release from muscovite is about two orders of magnitude greater than from K-feldspar (Fig. 12). Given that the difference in Sr concentration between K-feldspar and muscovite is one to two orders of magnitude, it is possible that muscovite dissolution has a discernible influence on $^{87}Sr/^{86}Sr$ of waters from RE.

$^{87}Sr/^{86}Sr$ was plotted against the amounts of K estimated to be released from dissolution of muscovite and K-feldspar respectively (Figs. 14 and 15). As expected, there are no significant relationships for RW waters. This confirms that variability in $^{87}Sr/^{86}Sr$ of these waters can be attributed primarily to variation in $^{87}Sr/^{86}Sr$ of carbonate minerals in the catchment. For RE waters, however, $^{87}Sr/^{86}Sr$ increases logarithmically with the K input from muscovite, and linearly (and more

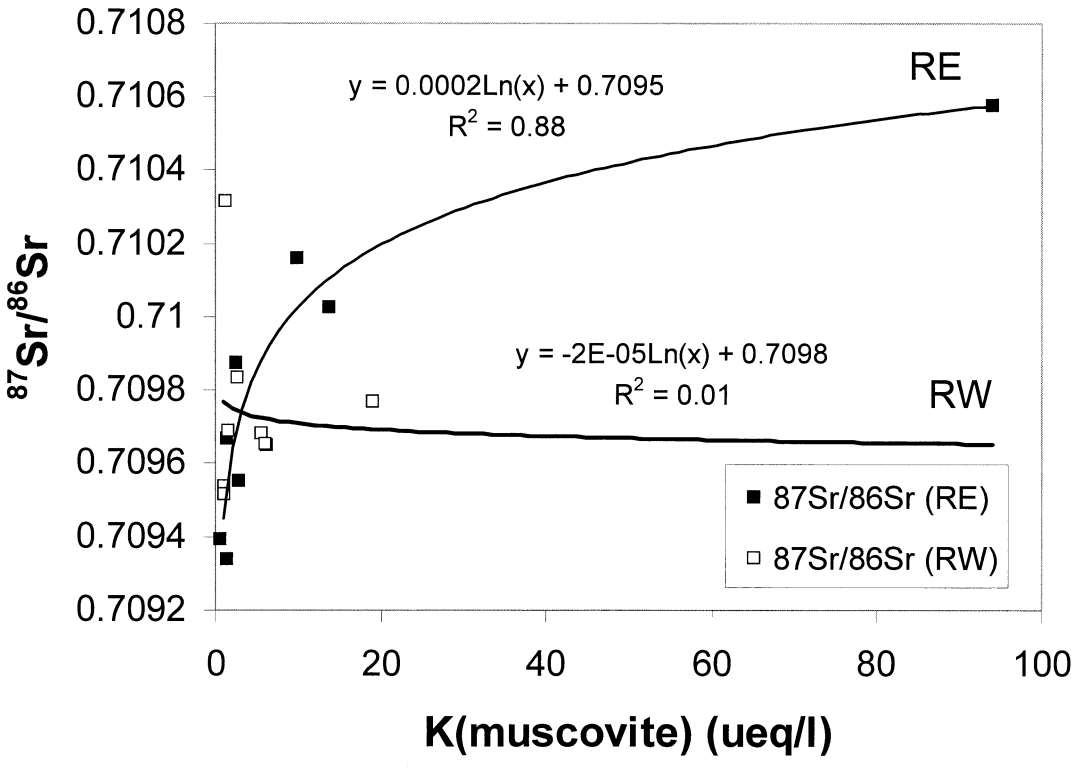

Fig. 14. $^{87}Sr/^{86}Sr$ in Robertson Glacier meltwaters as a function of the estimated amount of K derived from dissolution of muscovite (data from RE and RW displayed separately). Linear, logarithmic, exponential, and power law regressions were computed for each data set, and the regression that yielded the highest r^2 value is displayed.

strongly) with the K input from K-feldspar. This might indicate that the variability in $^{87}Sr/^{86}Sr$ of RE waters is attributable primarily to variability in the Sr input from K-feldspar. However, this argument is hard to sustain. Although the slope of the relationship between K (K-feldspar) and the total cation content of the waters is identical for RE and RW waters, $^{87}Sr/^{86}Sr$ of RW waters is apparently unrelated to K (K-feldspar). Furthermore, for a given value of $^{87}Sr/^{86}Sr$, K (K-feldspar) is greater in RW than in RE (Fig. 15). Given that rates of release of K from muscovite are an order of magnitude higher in RE than in RW, the variability in $^{87}Sr/^{86}Sr$ of RE waters is more likely to be controlled by the input of radiogenic Sr from muscovite. However, it should be remembered that only 3 or 4 samples show the elevated $^{87}Sr/^{86}Sr$ values that indicate a discernible influence from muscovite dissolution. Thus, the relationship between $^{87}Sr/^{86}Sr$ and K (K-feldspar) in RE waters may be fortuitous and could arise simply because the release of K from both K-feldspars and muscovite increases with cation concentration.

A plot of $^{87}Sr/^{86}Sr$ against the ratio Na/K in meltwaters provides further evidence for the influence of muscovite dissolution on $^{87}Sr/^{86}Sr$ of RE waters (Fig. 16). Although muscovite typically contains $<1\%$ Na (Albuquerque, 1975), K-feldspars may contain several percentage Na (Smith, 1974). Furthermore, Na in K-feldspars can be concentrated in perthitic inclusions, which may dissolve preferentially over the K-feldspar (Brantley et al., 1998). Thus, high values of Na/K may be diagnostic of K-feldspar dissolution, whereas lower values are diagnostic of muscovite dissolution. Low values are probably also characteristic of carbonate dissolution, because Na/K is lowest ($\sim$0.2) in the most dilute meltwaters, for which calcite dissolution is the primary solute source (not shown). For $^{87}Sr/^{86}Sr$ less than $\sim$0.7099, $^{87}Sr/^{86}Sr$ increases with Na/K in waters from both RE and RW. For $^{87}Sr/^{86}Sr$ greater than $\sim$0.7099, $^{87}Sr/^{86}Sr$ increases as Na/K decreases. The four most radiogenic samples from RE, and the single most radiogenic sample from RW plot on the latter trend. This suggests that for $^{87}Sr/^{86}Sr$ less than $\sim$0.7099, the variability in $^{87}Sr/^{86}Sr$ is attributable primarily to either variability in $^{87}Sr/^{86}Sr$ of carbonate minerals or to mixing of Sr from carbonate and K-feldspars. For higher values of $^{87}Sr/^{86}Sr$, the input of Sr from muscovite dissolution becomes significant. This change is presumably a function of the relative dissolution kinetics of muscovite, K-feldspar, calcite and dolomite, and the manner in which these change over time as a function of the saturation state of waters relative to these minerals.

5. CONCLUSIONS

Variations in the processes of chemical weathering by meltwaters draining from Robertson Glacier are linked to variations in the duration of contact between meltwaters and subglacial sediment. As contact time increases, there is a progressive shift from calcite dissolution by use of protons supplied by dissociation of carbonic acid to dolomite dissolution by using protons supplied by sulfide oxidation. This process shift is probably

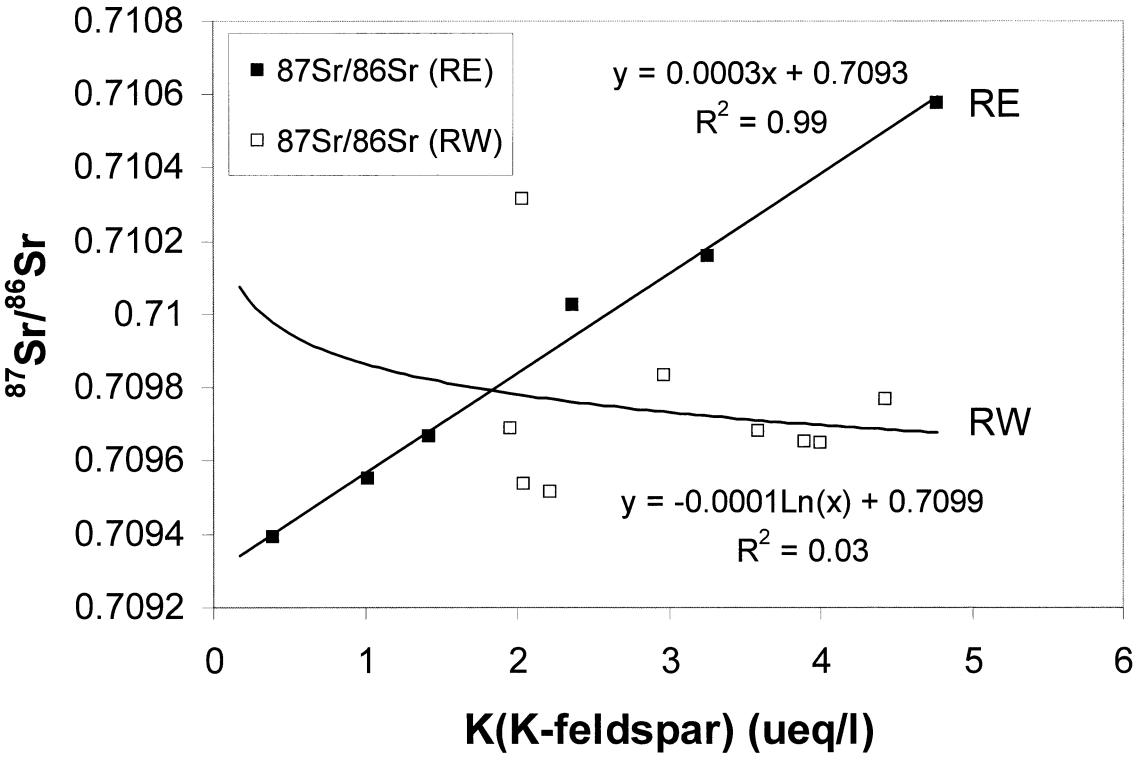

Fig. 15. $^{87}Sr/^{86}Sr$ in Robertson Glacier meltwaters as a function of the estimated amount of K derived from dissolution of K-feldspar (data from RE and RW displayed separately). Linear, logarithmic, exponential, and power law regressions were computed for each data set, and the regression that yielded the highest r^2 value is displayed.

linked to a difference in the nature of the predominant drainage pathway that meltwaters have followed, from major subglacial channels to some form of distributed drainage system.

Strontium concentration increases with cation concentration in both meltwater streams, but $^{87}Sr/^{86}Sr$ only does so in RE. In RW, $^{87}Sr/^{86}Sr$ values imply a predominantly carbonate source for Sr, whereas in RE, muscovite dissolution is also an identifiable source, which is especially significant for the more concentrated waters. In both streams, the influence of K-feldspar dissolution on $^{87}Sr/^{86}Sr$ seems to be more obvious at intermediate solute concentrations. The high relative importance of muscovite dissolution in the RE catchment seems to be linked to distinctive bedrock geology. Although muscovite seems to weather more rapidly than K-feldspar in this environment, its low Sr content means that it only affects $^{87}Sr/^{86}Sr$ in the most concentrated waters. A reduction in rates of carbonate weathering, relative to K-silicate weathering, as concentrated waters approach saturation with respect to carbonate minerals may also enhance its impact on $^{87}Sr/^{86}Sr$ of these waters. Nonstoichiometric release of $^{87}Sr/^{86}Sr$ and preferential release of Sr over K may occur where waters experience contact with freshly abraded mineral surfaces. Both these effects may help to explain why concentrated waters draining slowly into RE from a distributed subglacial drainage system are especially radiogenic. Crushing and grinding of bedrock are active processes in such environments, and maintain a continuous supply of freshly ground surfaces. In major subglacial drainage channels, however, water:rock contact times are short, and crushing and grinding are no longer active. Chemical weathering in this environment may attack primarily suspended sediment that has previously been depleted in surface cations (especially Sr with a high $^{87}Sr/^{86}Sr$) during an earlier phase of weathering in an environment where crushing and grinding were active.

Our results strongly suggest that in this predominantly carbonate catchment, the flux weighted mean isotopic composition of Sr in glacial runoff will closely resemble that of local carbonate bedrock. Sr with high $^{87}Sr/^{86}Sr$ is released during the weathering of muscovite and K-feldspar. However, the rapid dissolution kinetics of carbonate minerals ensure that the carbonate contribution to the Sr flux in runoff dominates at times of high discharge when waters are dilute and meltwater residence times within the glacier are low. The muscovite contribution to the Sr flux is more important, and has a discernible impact on the isotopic composition of Sr, at times of low discharge when meltwater-rock contact times are much longer and waters have passed through an environment where bedrock crushing and grinding are active. However, solute fluxes in glacial meltwater streams are usually dominated by transport under peak runoff conditions (e.g., Sharp et al., 1995) and it is unlikely that waters which have higher $^{87}Sr/^{86}Sr$ values represent a large fraction of bulk runoff. This suggests that even though glacially-enhanced release of Sr with high $^{87}Sr/^{86}Sr$ does occur from silicate minerals in carbonate terrains, it is unlikely to be an important factor in explaining the apparent links between the $^{87}Sr/^{86}Sr$ record in marine limestones and the extent of global glaciation.

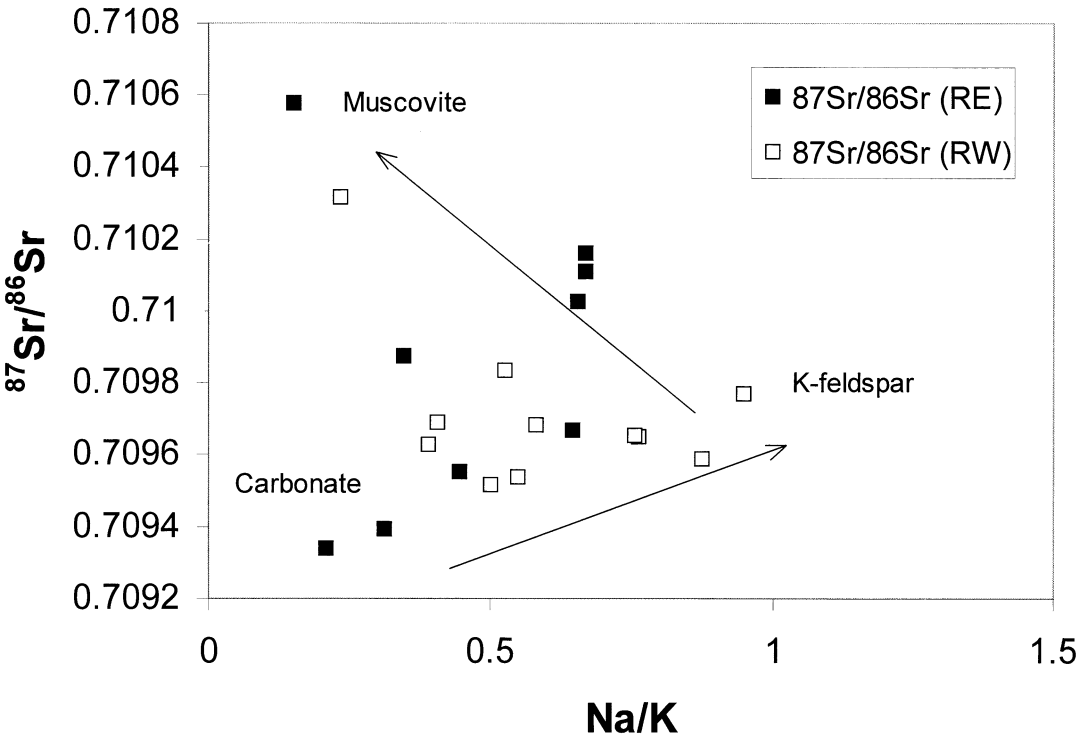

Fig. 16. $^{87}Sr/^{86}Sr$ in Robertson Glacier meltwaters as a function of the ratio (Na/K) (data from RE and RW displayed separately). Arrows indicate hypothetical weathering pathways representing the varying contributions of carbonate, K-feldspar, and muscovite dissolution to the Sr load of the meltwaters.

Acknowledgments—This work was supported by grants from NSERC (Canada) and the Royal Canadian Geographical Society. Permission to carry out fieldwork was kindly granted by Alberta Environmental Protection (Kananaskis Country). We are grateful to the staff of the University of Calgary Kananaskis Field Station for logistic support. We thank Joel Barker, Ian Fairchild, Scott Lamoureux, George Morris, Rod Smith, and John Woodward for field assistance, Pat Cavell for advice on the leaching process, Olga Levner for laboratory assistance, and John Duke for INAA analyses. Martyn Tranter and Hans Machel provided helpful comments on an earlier draft. We are grateful to two anonymous reviewers and to Thomas Bullen, whose constructive and insightful comments motivated the analysis of the relative importance of muscovite and K-feldspar dissolution.

Associate editor: E. H. Oelkers

REFERENCES

Albuquerque C. A. R. (1975) Partition of trace elements in co-existing biotite, muscovite and potassium feldspar of granitic rocks, northern Portugal. *Chem. Geol.* **16,** 89–108.

Anderson S. P., Drever J. I., and Humphrey N. F. (1997) Chemical weathering in glacial environments. *Geology* **25,** 399–402.

Anderson S. P., Drever J. I., Frost C. D., and Holden P. (2000) Chemical weathering in the foreland of a retreating glacier. *Geochim. Cosmochim. Acta* **64,** 1173–1189.

Blum J. D., Erel Y., and Brown K. (1994) $^{87}Sr/^{86}Sr$ ratios of Sierra Nevada stream waters: Implications for relative mineral weathering rates. *Geochim. Cosmochim. Acta* **58,** 5019–5025.

Blum J. D. and Erel Y. (1995) A silicate weathering mechanism linking increases in marine $^{87}Sr/^{86}Sr$ with global glaciation. *Nature* **373,** 415–418.

Blum A. E. and Stillings L. (1995) Feldspar dissolution kinetics. In *Chemical Weathering Rates of Silicate Minerals* (eds. A. F. White and S. L. Brantley), pp. 291–351. Reviews in Mineralogy 31. Mineralogical Society of America.

Blum J. D. and Erel Y. (1997) Rb-Sr isotope systematics of a granitic soil chronosequence: The importance of biotite weathering. *Geochim. Cosmochim. Acta* **61,** 3193–3204.

Blum J. D., Gazis C. A., Jacobson A. D., and Chamberlain C. P. (1998) Carbonate versus silicate weathering in the Raikhot watershed within the High Himalayan Crystalline Series. *Geology* **26,** 411–414.

Brantley S. L., Chesley J. T., and Stillings L. L. (1998) Isotopic ratios and release rates of strontium measured from weathering feldspars. *Geochim. Cosmochim. Acta* **62,** 1493–1500.

Brown G. H., Sharp M., Tranter M., Gurnell A. M., and Nienow P. W. (1994) Impact of post-mixing reactions on the major ion chemistry of bulk meltwaters draining the Haut Glacier d'Arolla, Valais, Switzerland. *Hydrol. Proc.* **8,** 465–480.

Brown G. H., Sharp M., and Tranter M. (1996) Subglacial chemical erosion: Seasonal variations in solute provenance, Haut Glacier d'Arolla, Valais, Switzerland. *Ann. Glaciol.* **22,** 25–31.

Bullen T., White A., Blum A., Harden J., and Schulz M. (1997) Chemical weathering of a soil chronosequence on granitoid alluvium: II. Mineralogic and isotopic constraints on the behavior of strontium. *Geochim. Cosmochim. Acta* **61,** 291–306.

Burke W. H., Denison R. E., Hetherington E. A., Koepnick R. B., Nelson H. F., and Otto J. B. (1982) Variation of seawater $^{87}Sr/^{86}Sr$ throughout Phanerozoic time. *Geology* **10,** 516–519.

Capo R. C. and DePaolo D. J. (1990) Seawater strontium isotope variations from 2.5 million years ago to the present. *Science* **249,** 51–55.

Cerny P. and Burt D. M. (1984) Paragenesis, crystallochemical characteristics, and geochemical evolution of micas in granitic pegmatites. In *Micas*(ed. S. W. Bailey), pp. 257–298. Reviews in Mineralogy 13. Mineralogical Society of America.

Chesley J. T., Quade J., and Ruiz J. (2000) The Os and. Sr isotopic record of Himalayan paleorivers: Himalayan tectonics and influence on ocean chemistry. *Earth Planet. Sci. Lett.* **179,** 115–124.

Claypool G. E. Holser W. T., Kaplan I. R., Sakai M., and Zak. I. (1980)

The age curves of sulfur and oxygen isotopes in marine sulfate and their mutual interpretation. *Chem. Geol.* **28,** 199–260.

Clow D. W., Mast A. M., Bullen T. D., and Turk J. T. (1997) Strontium 87/strontium 86 as a tracer of mineral weathering reactions and calcium sources in an alpine/subalpine watershed, Loch Vale, Colorado. *Water Res. Res.* **33,** 1335–1351.

Derry L. A. and France-Lanord C. (1996) Neogene Himalayan weathering history and river $^{87}Sr/^{86}Sr$: Impact on the marine Sr record. *Earth Planet. Sci. Lett.* **142,** 59–74.

Edmond J. M. (1992) Himalayan tectonics, weathering processes, and the strontium isotope record in marine limestones. *Science* **258,** 1594–1597.

English N. B., Quade J., DeCelles P. G., and Garzione C. N. (2000) Geologic control of Sr and major element chemistry in Himalayan rivers, Nepal. *Geochim. Cosmochim. Acta* **64,** 2549–2566.

Galy A., France-Lanord C., and Derry L. A. (1999) The strontium isotope budget of Himalayan rivers in Nepal and Bangladesh. *Geochim. Cosmochim. Acta* **63,** 1905–1925.

Hallet B. (1976) Deposits formed by subglacial precipitation of $CaCO_3$. *GSA Bull.* **85,** 1003–1015.

Harris N. (1995) Significance of weathering Himalayan metasedimentary rocks and leucogranites for the Sr isotope evolution of seawater during the early Miocene. *Geology* **23,** 795–798.

Harris N., Bickle M., Chapman H., Fairchild I., and Bunbury J. (1998) The significance of Himalayan rivers for silicate weathering rates: Evidence from the Bhote Kosi tributary. *Chem. Geol.* **144,** 205–220.

Heemskerk R. A. (1993a) Sulphur 34/32 determination. Technical procedure 26.0. Environmental Isotope Laboratory, University of Waterloo.

Heemskerk R. A. (1993b) Sulphate ^{18}O by combustion in metallic foil. Technical procedure 31.0. Environmental Isotope Laboratory, University of Waterloo.

Hodell D. A., Mead G. A., and Mueller P. A. (1990) Variation in the strontium isotope composition of seawater (8 Ma to present): Implications for chemical weathering rates and dissolved fluxes to the oceans. *Chem. Geol.* **80,** 291–307.

Holmden C., Creaser R. A., Muehlenbachs K., Leslie S. A., and Bergstrom S. M. (1996) Isotopic and elemental systematics of Sr and Nd in 454 Ma biogenic apatites: Implications for paleoseawater studies. *Earth Planet. Sci. Lett.* **142,** 425–437.

Karim A. and Veizer J. (2000) Weathering processes in the Indus River Basin: Implications from riverine carbon, sulfur, oxygen and strontium isotopes. *Chem. Geol.* **170,** 153–177.

Krishnaswami S., Trivedi J. R., Sarin M. M., Ramesh R., and Sharma K. K. (1992) Strontium isotopes and rubidium in the Ganga–Brahmaputra river system: Weathering in the Himalaya, fluxes to the Bay of Bengal and contributions to the evolution of oceanic $^{87}Sr/^{86}Sr$. *Earth Planet. Sci. Lett.* **109,** 243–253.

Krouse H. R. (1980) Sulfur isotopes in our environment. In *Handbook of Environmental Isotope Geochemistry: The Terrestrial Environment,* Vol. 1 (eds. P. Fritz and J. Fontes), pp. 22–44. Elsevier.

Machel H. G. and Cavell P. A. (1999) Low-flux, tectonically induced squeegee fluid flow ("hot flash") into the Rocky Mountain Foreland Basin. *Bull. Can. Petrol. Geol.* **47,** 510–533.

McMechan M. E. (1988) *Geology of Peter Lougheed Provincial Park, Rocky Mountain Front Ranges, Alberta.*Open File Report 2057. Geological Survey of Canada.

Palmer M. R. and Edmond J. M. (1989) The strontium isotope budget of the modern ocean. *Earth Planet. Sci. Lett.* **92,** 11–26.

Palmer M. R. and Edmond J. M. (1992) Controls over the strontium isotope composition of river water. *Geochim. Cosmochim. Acta* **56,** 2099–2111.

Probst A., El Ch'mari A., Aubert D., Fritz B., and McNutt R. (2000) Strontium as a tracer of weathering processes in a silicate catchment polluted by acid atmospheric inputs, Strengbach, France. *Chem. Geol.* **170,** 203–219.

Quade J., Roe I., DeCelles P. G., and Ohja T. P. (1997) The Late Neogene $^{87}Sr/^{86}Sr$ record of lowland Himalayan rivers. *Science* **276,** 1828–1831.

Raymo M. E., Ruddiman W. F., and Froelich P. N. (1988) Influence of late Cenozoic mountain building on ocean geochemical cycles. *Geology* **16,** 649–653.

Raymo M. E. and Ruddiman W. F. (1992) Tectonic forcing of late Cenozoic climate. *Nature* **359,** 117–122.

Richter F. M., Rowley D. B., and DePaolo D. J. (1992) Sr isotope evolution of seawater: The role of tectonics. *Earth Planet. Sci. Lett.* **109,** 11–23.

Röthlisberger H. (1972) Water pressure in intra- and subglacial channels. *J. Glaciol.* **11,** 177–203.

Sharp M., Tranter M., Brown G. H., and Skidmore M. (1995) Rates of chemical denudation and CO_2 drawdown in a glacier-covered alpine catchment. *Geology* **23,** 61–64.

Singh S. K., Trivedi J. R., Pande K., Ramesh R., and Krishnaswami S. (1998) Chemical and strontium, oxygen, and carbon isotopic compositions of carbonates from the Lesser Himalaya: Implications to the strontium isotopic composition of the source waters of the Ganga, Ghaghara, and the Indus rivers. *Geochim. Cosmochim. Acta* **62,** 743–755.

Smith J. V. (1974) *Feldspar Minerals. 2. Chemical and Textural Properties*. Springer-Verlag.

Speer J. A. (1984) Micas in igneous rocks. In *Micas* (ed. S. W. Bailey), pp. 299–349. Reviews in Mineralogy 13. Mineralogical Society of America.

Stillings L. and Brantley S. L. (1995) Feldspar dissolution at 25°C and pH 3: Reaction stoichiometry and the effect of cations. *Geochim. Cosmochim. Acta* **59,** 1483–1496.

Taylor A. S., Blum J. D., and Lasaga A. C. (2000a) The dependence of labradorite dissolution and Sr isotope release rates on solution saturation state. *Geochim. Cosmochim. Acta* **64,** 2389–2400.

Taylor A. S., Blum J. D., Lasaga A. S., and MaCinnis I. N. (2000b) Kinetics of dissolution and Sr release during biotite and phlogopite weathering. *Geochim. Cosmochim. Acta* **64,** 1191–1208.

Tessier A., Campbell P. G. C., and Bisson M. (1979) Sequential extraction procedure for the speciation of particulate trace metals. *Anal. Chem.* **51,** 844–851.

Tranter M., Sharp M. J., Lamb H. R., Brown G. H., Hubbard B. P., and Willis I. C. (in press) Geochemical weathering at the bed of Haut Glacier d'Arolla, Switzerland—A new model. *Hydrol. Proc.*

van Stempvoort D. R. and Krouse H. R. (1994) Controls of ^{18}O in sulfate: Review of geochemistry of sulfide oxidation. In *ACS Symposium Series 550*(eds. C. N. Alpers and D. W. Blowes), pp. 446–480. American Chemical Society.

Wadleigh M. A., Veizer J., and Brooks C. (1985) Strontium and its isotopes in Canadian rivers: Fluxes and global implications. *Geochim. Cosmochim. Acta* **49,** 1727–1736.

Walder J. S. and Hallet B. (1979) Geometry of former subglacial water channels and cavities. *J. Glaciol.* **23,** 335–346.

Yonge C. J. Goldberg L., and Krouse H. R. (1989) An isotope study of water bodies along a traverse of southwestern Canada. *J. Hydrol.* **106,** 245–255.

Zachos J. C., Opdyke B. N., Quinn T. M., Jones C. E., and Halliday A. N. (1999) Early Cenozoic glaciation, Antarctic weathering, and seawater $^{87}Sr/^{86}Sr$: Is there a link? *Chem. Geol.* **161,** 165–180.